Since January 2020 Elsevier has created a COVID-19 resource centre with free information in English and Mandarin on the novel coronavirus COVID-19. The COVID-19 resource centre is hosted on Elsevier Connect, the company's public news and information website.

Computational Biology and Chemistry 104 (2023) 107768

Contents lists available at ScienceDirect

Computational Biology and Chemistry

journal homepage: www.elsevier.com/locate/cbac

Dual computational and biological assessment of some promising nucleoside analogs against the COVID-19-Omicron variant

Mohnad Abdalla [a,**,1], Amgad M. Rabie [b,c,*,2,3]

[a] Key Laboratory of Chemical Biology (Ministry of Education), Department of Pharmaceutics, School of Pharmaceutical Sciences, Cheeloo College of Medicine, Shandong University, 44 Cultural West Road, Shandong Province 250012, PR China
[b] Dr. Amgad Rabie's Research Lab. for Drug Discovery (DARLD), Mansoura City 35511, Mansoura, Dakahlia Governorate, Egypt
[c] Head of Drug Discovery & Clinical Research Department, Dikernis General Hospital (DGH), Magliss El-Madina Street, Dikernis City 35744, Dikernis, Dakahlia Governorate, Egypt

ARTICLE INFO

Keywords:
Anti-Omicron-BA.5 agent
Anti-COVID-19 medication
Coronaviral-2 RNA-dependent RNA polymerase (RdRp)
SARS-CoV-2 proofreading 3′-to-5′ exoribonuclease (ExoN)
Polymerase inhibitor
Nucleos(t)ide analog
Riboprine/Forodesine
Nucleic acid ligand

ABSTRACT

Nucleoside analogs/derivatives (NAs/NDs) with potent antiviral activities are now deemed very convenient choices for the treatment of coronavirus disease 2019 (COVID-19) arisen by the severe acute respiratory syndrome coronavirus 2 (SARS-CoV-2) infection. At the same time, the appearance of a new strain of SARS-CoV-2, the Omicron variant, necessitates multiplied efforts in fighting COVID-19. Counteracting the crucial SARS-CoV-2 enzymes RNA-dependent RNA polymerase (RdRp) and 3′-to-5′ exoribonuclease (ExoN) jointly altogether using the same inhibitor is a quite successful new plan to demultiplicate SARS-CoV-2 particles and eliminate COVID-19 whatever the SARS-CoV-2 subtype is (due to the significant conservation nature of RdRps and ExoNs in the different SARS-CoV-2 strains). Successive *in silico* screening of known NAs finally disclosed six different promising NAs, which are riboprine/forodesine/tecadenoson/nelarabine/vidarabine/maribavir, respectively, that predictably can act through the planned dual-action mode. Further *in vitro* evaluations affirmed the anti-SARS-CoV-2/anti-COVID-19 potentials of these NAs, with riboprine and forodesine being at the top. The two NAs are able to effectively antagonize the replication of the new virulent SARS-CoV-2 strains with considerably minute *in vitro* anti-RdRp and anti-SARS-CoV-2 EC_{50} values of 189 and 408 nM for riboprine and 207 and 657 nM for forodesine, respectively, surpassing both remdesivir and the new anti-COVID-19 drug molnupiravir. Furthermore, the favorable structural characteristics of the two molecules qualify them for varied types of isosteric and analogistic chemical derivatization. In one word, the present important outcomes of this comprehensive dual study revealed the anticipating repurposing potentials of some known nucleosides, led by the two NAs riboprine and forodesine, to successfully discontinue the coronaviral-2 polymerase/exoribonuclease interactions with RNA nucleotides in the SARS-CoV-2 Omicron variant (BA.5 sublineage) and accordingly alleviate COVID-19 infections, motivating us to initiate the two drugs' diverse anti-COVID-19 pharmacological evaluations to add both of them betimes in the COVID-19 therapeutic protocols.

1. Introduction

In the last three years (2020–2022) since the severe acute respiratory syndrome coronavirus 2 (SARS-CoV-2) pandemic erupted across the globe, we and our multinational multidisciplinary research team have been in our laboratories day and night investigating and surveying coronavirus disease 2019 (COVID-19) patients of different ethnicities and ages, designing novel drugs to fight the virus, repurposing known medications to mitigate the pathologic effects of the disease, and exchanging our relevant insights and visions with co-experts in countries like Egypt, China, USA, Portugal, South Africa, and India. There are three logic and essential demands that have yet been adequately met for

* Correspondence to: 16 Magliss El-Madina Street, Dikernis City 35744, Dikernis, Dakahlia Governorate, Egypt.
** Corresponding author.
E-mail addresses: mohnadabdalla200@gmail.com (M. Abdalla), dr.amgadrabie@gmail.com, amgadpharmacist1@yahoo.com (A.M. Rabie).
[1] ORCID iD: 0000-0002-1682-5547
[2] ORCID iD: 0000-0003-3681-114X
[3] Co-first author and principal corresponding author.

https://doi.org/10.1016/j.compbiolchem.2022.107768
Received 16 May 2022; Received in revised form 16 August 2022; Accepted 4 September 2022
Available online 7 September 2022

the effective and successful management of COVID-19 disease; first one, potent antiviral medications that significantly limit SARS-CoV-2 transmission, cell entry, replication, and pathogenicity, second one, medications that attenuate the acute nonproductive immune response and thus considerably decrease end-organ damage, and third one, medications that have direct strong antifibrotic effects in patients with acute respiratory distress syndrome (ARDS) and thus combat the long-term sequelae of the COVID-19 (Chitalia and Munawar, 2020; Wang et al., 2020; Kaur et al., 2021; Rabie, 2021a, 2021b; Ip et al., 2021; Tardif et al., 2021). Compounds and drugs that act to satisfy mainly the first need of the three ones are relatively few to date. Of them, only nucleoside analogs/derivatives (NAs/NDs) and polyphenolics (PPhs) have shown significant successful progress as coronaviral-2 inhibitors (Mahase, 2021; Imran et al., 2021; Moirangthem and Surbala, 2021; Yan and Muller, 2020; Brunotte et al., 2021; Rabie, 2022a, 2022b; Cai et al., 2020; Rabie, 2021c, 2021d, 2021e; Raj et al., 2022, 2021). NAs are naturally more promising and highly biotolerated as antiviral therapeutics (Chien et al., 2020). Some new and repositioned efficacious nucleoside-like compounds are nowadays (and/or since 2020) under vast pharmacological and clinical investigations to be esteemed as effective potential anti-SARS-CoV-2/anti-COVID-19 medicines, *e.g.*, nirmatrelvir (Mahase, 2021), molnupiravir (Imran et al., 2021), remdesivir (Moirangthem and Surbala, 2021), GS-441524 (Yan and Muller, 2020; Brunotte et al., 2021), GS-443902 (Moirangthem and Surbala, 2021; Yan and Muller, 2020; Brunotte et al., 2021), cordycepin (Rabie, 2022a), didanosine (Rabie, 2022b), and favipiravir (Cai et al., 2020).

The frightening SARS-CoV-2 Omicron variant, also known as B.1.1.529 (or, simply, BA), first began its tear around the world late 2021, and now has more than five sisters of BA sublineages, *e.g.*, BA.1, BA.2, BA.3, BA.4, and BA.5 (World Health Organization, 2022). South African scientists announced the new variant on November 24, 2021, immediately after its first appearance (World Health Organization, 2022). As of nearly the beginning of July 2022, this highly infectious and new variant had been reported to be detected in more than 200 countries (World Health Organization, 2022). Omicron variant constructure has several modifications as compared to the constructure of its original predecessor (The Washington Post, 2022). The majority of these mutations are located in its spike (S) proteins (The Washington Post, 2022). Being unfixed and changeable day by day from one strain to the newer, spike protein is not that attractive target for designing new therapies against SARS-CoV-2 variants. While, on the other hand, targeting the universal fixed proteins among all variants, *e.g.*, SARS-CoV-2 replication RNA-dependent RNA polymerase (RdRp) and proofreading 3′-to-5′ exoribonuclease (ExoN) enzymes, through repurposing known compounds is much more effective and time-saving approach in this battle, even against the expectedly coming resistant coronaviral-2 strains. Moreover, therapies targeting the spike protein have only one chance to fight the coronaviral infection, since after passage of any viral particles inside the host body (or if these therapies were taken after the occurrence of the infection) there will not be any further abilities of these therapies to stop virus propagation and infection. Unlike therapies targeting the replication and proofreading enzymes, which have unlimited number of continuous chances to fight the virus and its successors, and prevent their further multiplication throughout the entire human body (even if these therapies were taken after the occurrence of the infection). In the first weeks of 2022, we as a multidisciplinary team continued our scientific journey and worked around the clock to discover effective anti-SARS-CoV-2-Omicron-variant drug candidates.

Tactical nucleoside analogism is among the favorable therapeutic choices in drug designers' and pharmaceutical chemists' brains to fight and stop the coronavirus multiplication inside the human body (Imran et al., 2021; Moirangthem and Surbala, 2021; Yan and Muller, 2020; Brunotte et al., 2021; Rabie, 2022a, 2022b; Cai et al., 2020; Chien et al., 2020). In this dual COVID-19 therapeutic tactic, the used nucleoside/-nucleotide analog makes use of its high similarity with the normal inbred nucleosides and nucleotides to effectively misguide and deceive the SARS-CoV-2 RdRp (the nonstructural protein complex 12/7/8 or nsp12-nsp7-nsp8) and ExoN (the nonstructural protein complex 14/10 or nsp14-nsp10) enzymes (Chien et al., 2020). Nsp12-nsp7-nsp8 and nsp14-nsp10 protein complexes are very indispensable enzymes in the replication/proofreading of the coronaviral-2 genome, and thus, their strong inhibition will significantly block the replication of SARS-CoV-2 particles. Nucleoside-like agents discompose both RdRp and ExoN enzymes through complete incorporation in the viral RNA genetic strands in place of the correct naturally-occurring nucleosides/nucleotides, resulting in repeated excessive ambiguous coding and premature termination of RNA synthesis with the formation of vague RNA strands at the end; these faulty strands represent abnormal noninfectious and inactive particles, hence there would not be any further multiplication of the virus (Rabie, 2022a, 2022b; Chien et al., 2020). Some of the aforementioned anti-COVID-19 agents, *e.g.*, molnupiravir and remdesivir (Fig. 1A) and their active metabolites, β-D-N^4-hydroxycytidine (NHC) and GS-441524, respectively, draw on this effective mechanism in their inhibitory and blocking activities on the SARS-CoV-2 particles (Imran et al., 2021; Moirangthem and Surbala, 2021; Yan and Muller, 2020; Brunotte et al., 2021). With the progressive evolution of more resistant new strains/variants/subvariants of SARS-CoV-2, discovering more potent and broad-spectrum natural or synthetic anti-SARS-CoV-2 drugs became a must.

In this presented research work, we have explored the combined inhibitory activities of some NAs on both SARS-CoV-2 RdRp and ExoN enzymes as a novel effective strategy to double combat COVID-19 (Khater et al., 2021). Few compounds, *e.g.*, the phytochemical biflavonoid metabolite isoginkgetin, were recently reported to act through an analogous strategy by hitting both SARS-CoV-2 RdRp and main protease (M^{pro}) enzymes instead (Raj et al., 2022). After screening of different libraries of nucleosides and NAs, we chose the top fifteen nucleoside-like compounds with the best results to construct a very small library of them specifically designed for our work (Fig. 1B). Computation-based molecular docking revealed that about six of these fifteen compounds showed very good binding free energies with both enzymes, SARS-CoV-2 RdRp and ExoN, compared to those of the two positive controls (references), remdesivir and molnupiravir, with the same two enzymes. However, the other compounds of the fifteen ones, *e.g.*, neplanocin A, tubercidin, and fludarabine, showed relatively moderate-to-good results. Molecular docking and dynamics simulations studies of the chosen six compounds disclosed the superiority of the two compounds riboprine and forodesine in hitting the catalytic active sites of both enzymes with the formation of much more stable complexes having higher negative binding free energies. Biological evaluations of the six NAs against both coronaviral-2 RdRp and ExoN proteins and against the entire SARS-CoV-2 Omicron variant particles demonstrated nearly the same interesting superiority of riboprine and forodesine, respectively.

Based on these current results and previous data (Zhao et al., 2022, 2021; Lin et al., 2021; Eissa et al., 2021), we can conclude that, first, riboprine and forodesine can be further *in vivo* and clinically investigated for repurposing against COVID-19 and, second, the expected potent clinical inhibitory effects of riboprine and forodesine against SARS-CoV-2 replication may be principally attributed to the triple synergistic inhibitory activities against the three enzymes RdRp, ExoN, and adenosine kinase (ADK), *i.e.*, may be closely related to the RdRp, ExoN, and ADK inhibitory activities of riboprine and forodesine. The possible SARS-CoV-2 RNA mutagenicity of both drugs, *via* nucleoside analogism mode of action and incorporation into the new coronaviral-2 RNA strands, should also be extensively and clinically studied. The pharmacokinetics of these drugs which we intend to try repurposing them against COVID-19 should be significantly put into account, because tissue distributions of these potential anticoronaviral-2 drugs will certainly affect their total capabilities of reducing viral loads of SARS-CoV-2 particles in COVID-19 therapy (Wang and Chen, 2020). The possibility of pharmaceutically formulating the promising

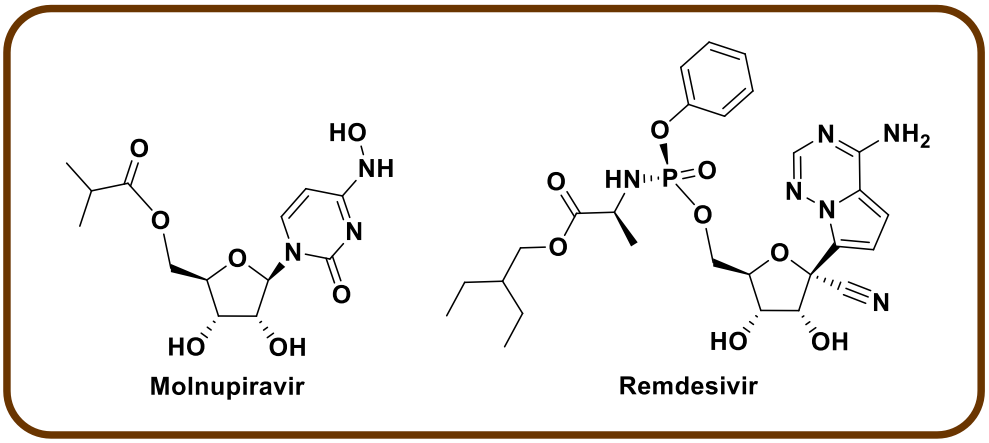

A

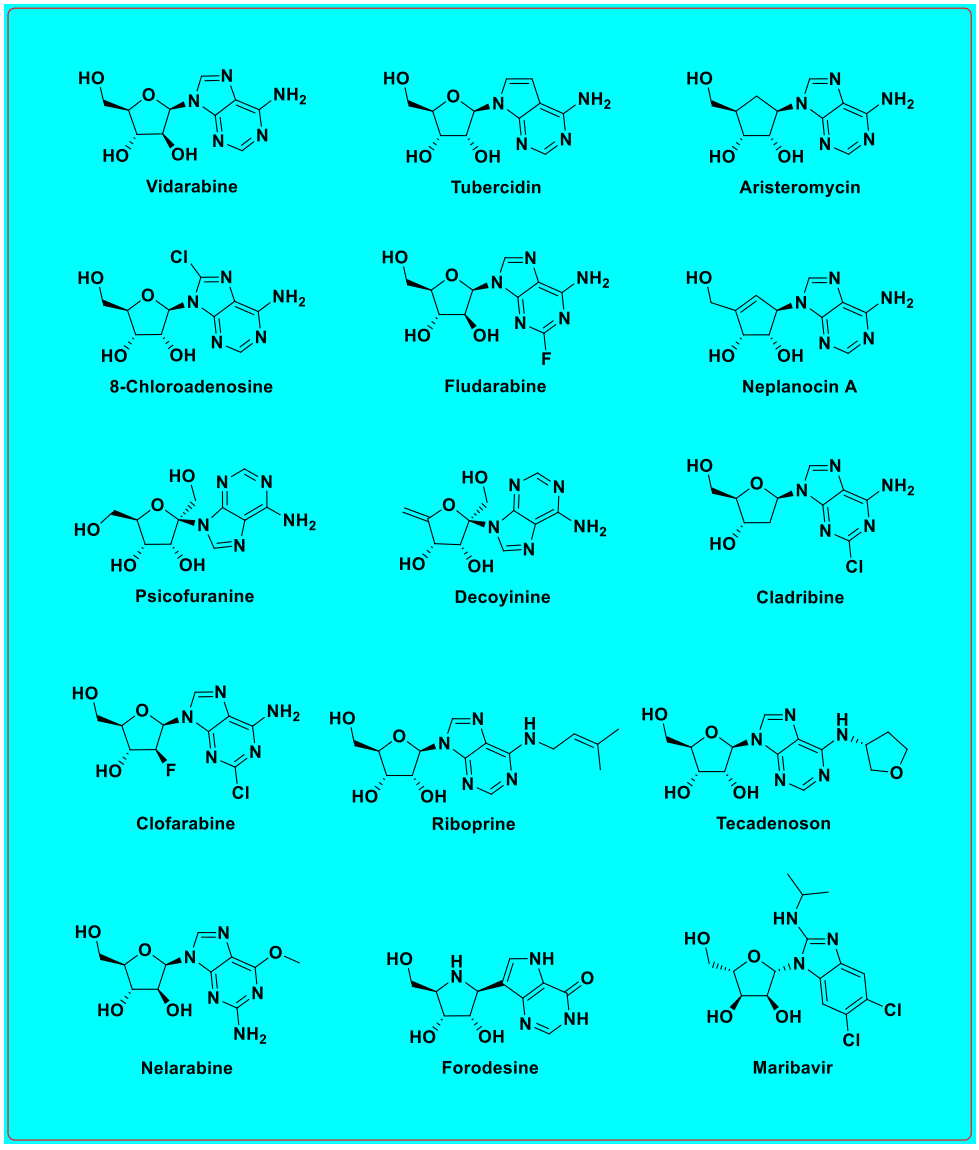

B

Fig. 1. Chemical molecular structures of: (**A**) Known anti-SARS-CoV-2/anti-COVID-19 medicines, molnupiravir and remdesivir. (**B**) Screened NAs as potential anti-SARS-CoV-2 agents (a small composed library).

nucleoside-like agents of the six tested ones as rapid-action nasal/oral anti-COVID-19 spray/drops should also be seriously considered.

2. Materials and methods

2.1. In silico computational evaluation

2.1.1. Targeted coronaviral-2 proteins preparation

The 3D structures of the target SARS-CoV-2 RdRp and ExoN proteins were obtained from the RCSB Protein Data Bank (PDB) with PDB identification codes 7BV2 and 7MC6, respectively. Both enzymatic proteins were obtained in the complex form with their protein cofactors (*i.e.*, were obtained cocrystallized in the nsp12-nsp7-nsp8 and nsp14-nsp10 complex forms, respectively) to increase nature simulation. The PDB files of the two proteins were properly downloaded. Proteins were viewed through PyMOL Molecular Graphics Visualizer 2.4 software (Schrödinger, LLC), and their predetected active site residues (with their closest neighboring residues) were then checked for complete presence and correctness. The catalytic active site residues highlighted through PyMOL software were noted for the planned *in silico* studies.

2.1.2. Diverse nucleosidic ligands selection and preparation

To choose the best NAs for the current study, a primary virtual screening of diverse libraries of hundreds of NAs was done against SARS-CoV-2 RdRp and ExoN proteins using the Molecular Operating Environment (MOE) platform (Chemical Computing Group). The fifteen NAs with the top collective results as the best hitting candidates of both proteins were selected to continue the long journey of this present research study. After this initial screening, an extensive literature survey was also performed for the study of the potentials of the chosen fifteen NAs as antivirals. Many of them have demonstrated strong antiviral capabilities either in computational or experimental studies or in both of them. This is one of the main reasons we have tried these potential inhibitors in the current virtual docking and simulation studies of SARS-CoV-2 RdRp and ExoN enzymes. The chemical structures of the selected NAs were adequately prepared and full optimized using ChemDraw Professional 16.0 software (licensed version) for the next *in silico* studies.

2.1.3. Molecular docking protocol

Blind docking of the fifteen selected NAs in SARS-CoV-2 RdRp and ExoN proteins was performed *via* MOE. Remdesivir (with its phosphate group unsubstituted, for better matching with the tested NAs) and molnupiravir were used as positive control anti-SARS-CoV-2 references having proven potent RdRp/ExoN inhibitory activities. Prior to starting these docking procedures, some important preparations (mainly, additions and corrections) were needed. All the missed atoms/residues in the SARS-CoV-2 RdRp and ExoN were added *via* MOE structure modeling. The two viral proteins were precisely prepared for molecular docking by the addition of hydrogen atoms using the 3D-protonation module of the used MOE software; any partial charges were also corrected for both proteins. RdRp and ExoN were energy minimized in their complex forms *via* the Amber-99 force field which is available in MOE. Similarly, the structures of the fifteen target ligands, remdesivir, and molnupiravir were also adequately energy minimized in MOE. For docking of the target/reference ligands with the two proteins, the known London-dG scoring functions were utilized for binding energy calculations. For each docked NA/reference molecule, the MOE software produced about twenty different poses with each docked SARS-CoV-2 protein. Of all the docking poses for each molecule with each protein, the one with the more best molecular interactions, *i.e.*, the top ranked pose, was recorded and saved. MOE gives a numerical value for the interaction of any potential ligand with any certain protein in the form of a docking S-score (docking scores are expressed in kcal/mol). This docking binding energy or S-score represents the net energy of the formed protein-ligand complex and it also primarily reflects the degree of its expected stability (*i.e.*, it provides a primary idea about the predicted stability of this formed complex prior to performing the more detailed robust computations *via* the molecular dynamics "MD" simulations). The molecular docking revealed six promising target NAs with very good S-scores compared to the two reference NAs (these top ranked NAs represent the core point of the current research). MOE software shows all the possible molecular interactions (of all types) made during the docking process; these include, *e.g.*, hydrogen bonding (H-bonds), hydrophobic interactions, ionic interactions/bonds, and salt bridges. A confirmative redocking study was conducted for the extravalidation and precision purpose of molecular docking outputs. For the best six target NAs and the two reference NAs, the 2D and 3D output images of all the produced protein-ligand complexes (showing almost all the possible interactions) were saved for both further investigative analysis and final scientific reporting.

2.1.4. Molecular dynamics (MD) simulation protocol

The six NAs ranked with the top results, *e.g.*, with the best molecular interactions, lowest docking score (S-score), and lowest root-mean-square deviation (RMSD), computed through MOE for both docked proteins (using their relevant apoenzymes as the standard proteins) were then employed for further *in silico* studies, mainly the MD simulation studies, using Schrödinger's Desmond module MD-Simulation software (Schrödinger Release 2021–4, licensed version). For MD simulation of the selected NAs, the best docking poses of these NAs in complexes with the SARS-CoV-2 RdRp and ExoN enzymes were kept in PDB format in MOE to be used for further virtual stability studies in Schrödinger's Desmond module. The built-in Desmond System Builder tool was used in this current protocol to create the solvated water-soaked MD-Simulation system. The TIP3P model was utilized as the solvating model in the present experiment. With periodic boundary conditions, an orthorhombic box was accurately adjusted with a good boundary distance of almost 10 Å from the outer surface of each of the two coronaviral-2 proteins. The simulation systems were neutralized of complex charges by the addition of a reasonably sufficient amount of counter ions. To retain the isosmotic conditions, 0.10 mol/L sodium and chloride ions, *i.e.*, 0.10 M NaCl, were added into the simulation panel. Prior to beginning the simulation process, a predefined equilibration procedure was done. The system of the MD simulation was equilibrated by employing the standard Desmond protocol at a constant pressure of about 1.0 bar and a constant temperature of 300 K (NPT ensemble; considering the viral nature of the two target enzymatic proteins), and also by employing the known Berendsen coupling protocol with one temperature group. Hydrogen atom bond length was properly constrained using the validated SHAKE algorithm. Particle Mesh Ewald (PME) summation method was used to specifically model long-range electrostatic interactions. On the other hand, an exact cutoff of 10 Å was specifically assigned for van der Waals and short-range electrostatic interactions. As previously mentioned, the MD simulation was run at ambient pressure conditions of 1.013 bar while the used temperature was exactly set to 300 K for each 100 nsec (ns) period of this MD simulation, and 1000 frames were saved into each simulation trajectory file. The simulation run time for each complex system and apo system was fixed to 100 ns as a total. After simulations, the trajectory files of the simulated systems were used for calculation of the various structural parameters required, *e.g.*, RMSD (Å), root-mean-square fluctuation (RMSF; Å), radius of gyration (rGyr; Å), number of protein-ligand contacts (# of total contacts), interactions fractions (%), intermolecular H-bonds (from all aspects), molecular surface area (MolSA; $Å^2$), solvent-accessible surface area (SASA; $Å^2$), and polar surface area (PSA; $Å^2$), to extensively perform stability studies of the complex and apo systems. The results of the most promising two compounds, riboprine and forodesine, were stored to be reported and debated in the present paper.

2.2. In vitro biological evaluation

2.2.1. Specifications of the bioassayed NAs

Riboprine (N^6-(2-Isopentenyl)adenosine, CAS Registry Number: 7724–76–7) was purchased from BenchChem (BENCH CHEMICAL, Austin, Texas, U.S.A.) (Catalog Number: B141774, Purity: ≥ 99 %). While forodesine (Immucillin-H, CAS Registry Number: 209799–67–7), nelarabine (Arranon, CAS Registry Number: 121032–29–9), tecadenoson (CVT-510, CAS Registry Number: 204512–90–3), maribavir (1263W94, CAS Registry Number: 176161–24–3), vidarabine (Arabinosyladenine "Ara-A", CAS Registry Number: 5536–17–4), remdesivir (GS-5734, CAS Registry Number: 1809249–37–3), and molnupiravir (EIDD-2801, CAS Registry Number: 2349386–89–4) were purchased from Biosynth Carbosynth (Carbosynth Ltd., Berkshire, U.K.) (for forodesine, Product Code: MD11591, Purity: ≥ 98 %; for nelarabine, Product Code: NN26176, Purity: ≥ 98 %; for tecadenoson, Product Code: EIA51290, Purity: ≥ 98 %; for maribavir, Product Code: AM178224, Purity: ≥ 98 %; for vidarabine, Product Code: NA06007, Purity: ≥ 98 %; for remdesivir, Product Code: AG170167, Purity: ≥ 98 %; for molnupiravir, Product Code: AE176721, Purity: ≥ 98 %). The ultrapure solvent dimethylsulfoxide (DMSO, CAS Registry Number: 67–68–5) was purchased from a local distributor, El-Gomhouria Company For Drugs (El-Gomhouria Co. For Trading Drugs, Chemicals & Medical Supplies, Mansoura Branch, Egypt) (Purity: ≥ 99.9 % "anhydrous").

2.2.2. In vitro anti-RdRp/anti-ExoN assay (SARS-CoV-2-RdRp-Gluc Reporter Assay) of the selected NAs

First, the used cells, 293T cells (ATCC CRL-3216), were kept in Dulbecco's modified Eagle's medium (DMEM; Gibco) with 10% (v/v) fetal bovine serum (FBS; Gibco), then they were cultured at 37 °C in a humidified atmosphere of CO_2 (5%). The HEK293T cells were transfected using Vigofect transfection reagents (Vigorous) according to the strict instructions of the manufacturer. The required plasmid DNAs, antibodies, and reagents were purchased and treated exactly as in the literature procedures (Zhao et al., 2022, 2021). The examined drugs/chemicals are as described in Subsection 2.2.1. Also, western blotting (for the collected transfected HEK293T cells), real-time RT-PCR (for the extracted total RNA of transfected HEK293T cells), and cell viability test (using Cell Counting Kit-8 (CCK8), Beyotime) were exactly performed as in the relevant typical methodologies of the literature (Zhao et al., 2022, 2021). The steps of the well-designed *in vitro* SARS-CoV-2-RdRp-Gluc Reporter Assay were accurately carried out according to the same original method of literature but with modifying almost all the proteins to be identical to the SARS-CoV-2 Omicron variant "B.1.1.529/BA.5 sublineage" (HEK293T cells were transfected in this biochemical assay with CoV-Gluc, nsp12, nsp7, and nsp8 plasmid DNAs at the ratio of 1:10:30:30, and with CoV-Gluc, nsp12, nsp7, nsp8, nsp10, and nsp14 plasmid DNAs at the ratio of 1:10:30:30:10:90) (Zhao et al., 2022, 2021). Exactly as instructed in the original assay, a stock of coelenterazine-h was dissolved in absolute ethanol (of very pure analytical grade) to a concentration of 1.022 mM (Zhao et al., 2022, 2021). Directly before each assay, the stock was diluted in phosphate-buffered saline (PBS) to a concentration of 16.7 μM and incubated in the dark for 30 min at room temperature (Zhao et al., 2022, 2021). For luminescence assay, 10 μL of the supernatant was added to each well of a white and opaque 96-well plate, then 60 μL of the 16.7 μM coelenterazine-h solution was injected, and luminescence was measured for 0.5 s using the Berthold Centro XS3 LB 960 microplate luminometer (Zhao et al., 2022, 2021). Final results were statistically represented as the mean (μ) ± the standard deviation (SD) from at least three independent experiments. Statistical analysis was performed using SkanIt 4.0 Research Edition software (Thermo Fisher Scientific) and Prism V5 software (GraphPad). All the resultant data were considered statistically significant at $p < 0.05$.

2.2.3. In vitro anti-SARS-CoV-2 and cytotoxic bioactivities multiassay of the selected NAs

This established *in vitro* anti-COVID-19 multiassay (including the cytotoxicity test), which was precisely designed for the valuation and rating of the pure anti-SARS-CoV-2 activities of potential anti-COVID-19 agents, is based mainly upon the authentic procedures of Rabie (Rabie, 2021b, 2021c, 2021d, 2021e, 2022a, 2022b). The complete procedures were carried out in a specialized biosafety level 3 (BSL-3) laboratory. The assayed new subvariant of SARS-CoV-2 virus, the newest Omicron sublineage (B.1.1.529/BA.5 sublineage), was isolated from the fresh nasopharynx aspirate and throat swab of a 22-year-old Portuguese girl with confirmed COVID-19 infection using Vero E6 cells (ATCC CRL-1586) on 2 May, 2022. The starting titer of the stock virus ($10^{7.25}$ $TCID_{50}$/mL) was prepared after three serial passages in Vero E6 cells in infection media (DMEM supplemented with 4.5 g/L D-glucose, 100 mg/L sodium pyruvate, 2% FBS, 100,000 U/L Penicillin-Streptomycin, and 25 mM *N*-(2-hydroxyethyl)piperazine-*N*′-ethanesulfonic acid (HEPES)). The tested target and reference NAs (along with the solvent DMSO) are as previously referred to in Subsection 2.2.1. Preliminary pilot assays were performed mainly to determine the best concentration of the tested NAs to begin the *in vitro* anti-SARS-CoV-2 and cytotoxicity tests with. Accordingly, the stocks of the tested compounds were precisely prepared by dissolving each of the eight compounds in DMSO to obtain a 100,000 nM (100 μM) concentration of each compound. Additionally, DMSO was used for the purpose of a negative control comparison to make this experimental study placebo-controlled. To assess the total *in vitro* anti-SARS-CoV-2 activity of each of the target drugs, riboprine, forodesine, nelarabine, tecadenoson, maribavir, and vidarabine, in comparison to that of each of the two positive control/reference drugs, remdesivir and molnupiravir, along with that of the negative control solvent, DMSO, Vero E6 cells were pretreated with each of the nine compounds diluted in infection media for 1 h prior to infection by the new Omicron variant of the SARS-CoV-2 virus at MOI = 0.02. The nine tested compounds were maintained with the virus inoculum during the 2-h incubation period. The inoculum was removed after incubation, and the cells were overlaid with infection media containing the diluted test compounds. After 48 h of incubation at 37 °C, supernatants were immediately collected to quantify viral loads by $TCID_{50}$ assay or quantitative real-time RT-PCR "qRT-PCR" (TaqMan Fast Virus 1-Step Master Mix). Viral loads in this assay were fitted in logarithm scale ($\log_{10}$ $TCID_{50}$/mL, $\log_{10}$ $TCID_{90}$/mL, and $\log_{10}$ viral RNA copies/mL), not in linear scale, under increasing concentrations of the tested compounds. Four-parameter logistic (4PL) regression (GraphPad Prism) was used to fit the dose-response curves and determine the EC_{50} and EC_{90} of the tested compounds that inhibit SARS-CoV-2 viral replication ($CPEIC_{100}$ was also determined for each compound). Cytotoxicity of each of the nine tested compounds was also evaluated in Vero E6 cells using the CellTiter-Glo Luminescent Cell Viability Assay (Promega). Final results were statistically represented as the $\mu \pm SD$ from at least three independent experiments. Statistical analysis was done using SkanIt 4.0 Research Edition software (Thermo Fisher Scientific) and Prism V5 software (GraphPad). All the produced data were considered statistically significant at $p < 0.05$.

3. Results and discussion

3.1. Computational molecular modeling of the selected NAs as potential anti-COVID-19 drugs

After computational screening and filtration of several libraries of nucleosides and NAs, the top fifteen nucleoside-like molecules with the best and most ideal pharmacodynamic/pharmacokinetic results concerning the foreseen anti-SARS-CoV-2 activities were selected for our specific duty. The chosen compounds were, respectively, as follows: riboprine, forodesine, tecadenoson, nelarabine, vidarabine, maribavir, neplanocin A, tubercidin, cladribine, decoyinine, aristeromycin,

Table 1
The binding energy values (docking S-scores) and the major noncovalent bond interactions estimated during molecular docking of the fifteen screened NAs against the two SARS-CoV-2 proteins, RdRp and ExoN enzymes (using remdesivir and molnupiravir as the positive control drugs), respectively. The fifteen NAs are arranged in a collective descending order, starting from the top sorted one and ending with the least sorted one, from the energetic/stability point of view.

Classification	Compound Name	Docking S-score (kcal/mol)		Major Noncovalent Bond Interactions	
		RdRp (7BV2)	ExoN (7MC6)	RdRp (7BV2)	ExoN (7MC6)
Screened NAs	Riboprine	-7.2	-7.9	Arg553, Arg555, Thr556, Ala558, Lys621, Cys622, Asp623, Arg624, Thr680, Ser681, Ser682, Thr687, Ala688, Asn691, Leu758, Ser759, Asp760, Asp761, Cys813	Asp90, Val91, Glu92, Gly93, Cys94, His95, Asn104, Pro141, Phe146, Leu149, Trp186, Ala187, Gly189, Phe190, Gln191, Asn252, Leu253, Gln254, His268, Asp273
	Forodesine	-7.4	-7.7		
	Tecadenoson	-7.2	-7.5		
	Nelarabine	-7.6	-7.0		
	Vidarabine	-7.3	-6.8		
	Maribavir	-6.5	-7.5		
	Neplanocin A	-7.2	-6.6		
	Tubercidin	-7.0	-6.7		
	Cladribine	-7.0	-6.7		
	Decoyinine	-6.3	-7.2		
	Aristeromycin	-6.1	-7.2		
	Fludarabine	-6.3	-6.9		
	Clofarabine	-6.2	-6.9		
	Psicofuranine	-6.2	-6.8		
	8-Chloroadenosine	-6.0	-7.0		
Reference Drugs	Remdesivir	-6.4	-7.0	Asp452, Lys545, Arg553, Arg555, Thr556, Val557, Ala558, Lys621, Asp623, Arg624, Thr680, Ser681, Ser682, Thr687, Ala688, Asn691, Leu758, Ser759, Asp760, Asp761, Cys813	Asp90, Val91, Glu92, Gly93, His95, Asn104, Pro141, Phe146, Leu149, Trp186, Ala187, Phe190, Gln191, Asn252, Leu253, Gln254, His268, Asp273
	Molnupiravir	-6.2	-7.2		

fludarabine, clofarabine, psicofuranine, and 8-chloroadenosine. A small new library was made of these fifteen compounds which are a mixture of natural and synthetic molecules (see Fig. 1B). In a next step, further molecular docking specifically against SARS-CoV-2 RdRp and ExoN revealed that the compounds riboprine, forodesine, tecadenoson, nelarabine, vidarabine, and maribavir, respectively, have the lowest and best inhibitory binding energies (ranged from −6.5 to −7.9 kcal/mol) compared to the two reference anti-RdRp/anti-ExoN drugs, remdesivir and molnupiravir (having binding energies ranged from −6.2 to −7.2 kcal/mol), as presented in Table 1. The catalytic pockets (*i.e.*, active sites) of the two coronaviral-2 enzymes, RdRp (which is the main enzyme responsible for replication and transcription of the coronaviral-2 RNA genome) and ExoN (it is worth mentioning that nsp14 or the proofreading exoribonuclease of SARS-CoV-2 has two active sites; the exoribonuclease active site, the major one that we are concerned with in the current study, and the methyltransferase active site), were nearly detected and validated through previous several computational, crystallographic, and biochemical experiments in the literature (Doharey et al., 2022; DrugDevCovid19, 2022a, 2022b; Moeller et al., 2022). Investigating and analyzing the resultant *in silico* interactions of the aforementioned six molecules with the residues of SARS-CoV-2 RdRp and ExoN proteins showed that all molecules significantly hit most of the active amino acid residues of the catalytic pockets of both enzymes with strong interactions, including, mainly, H-bonds, hydrophobic

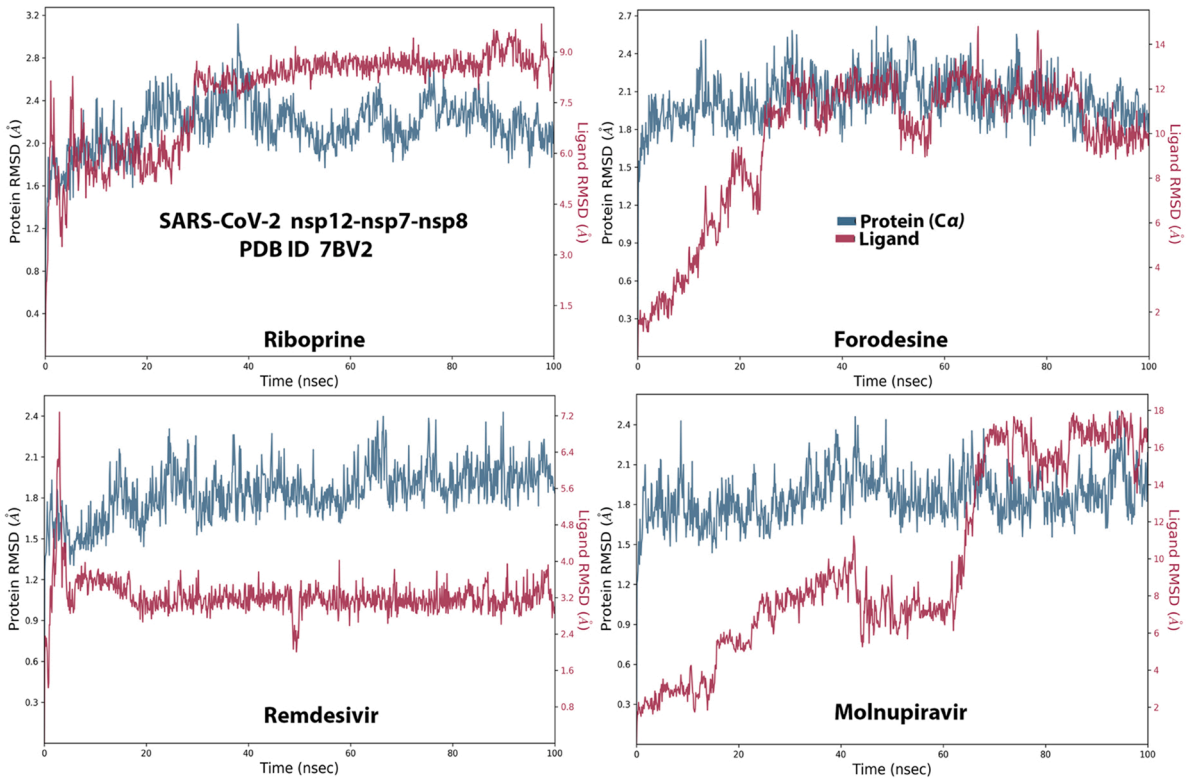

A

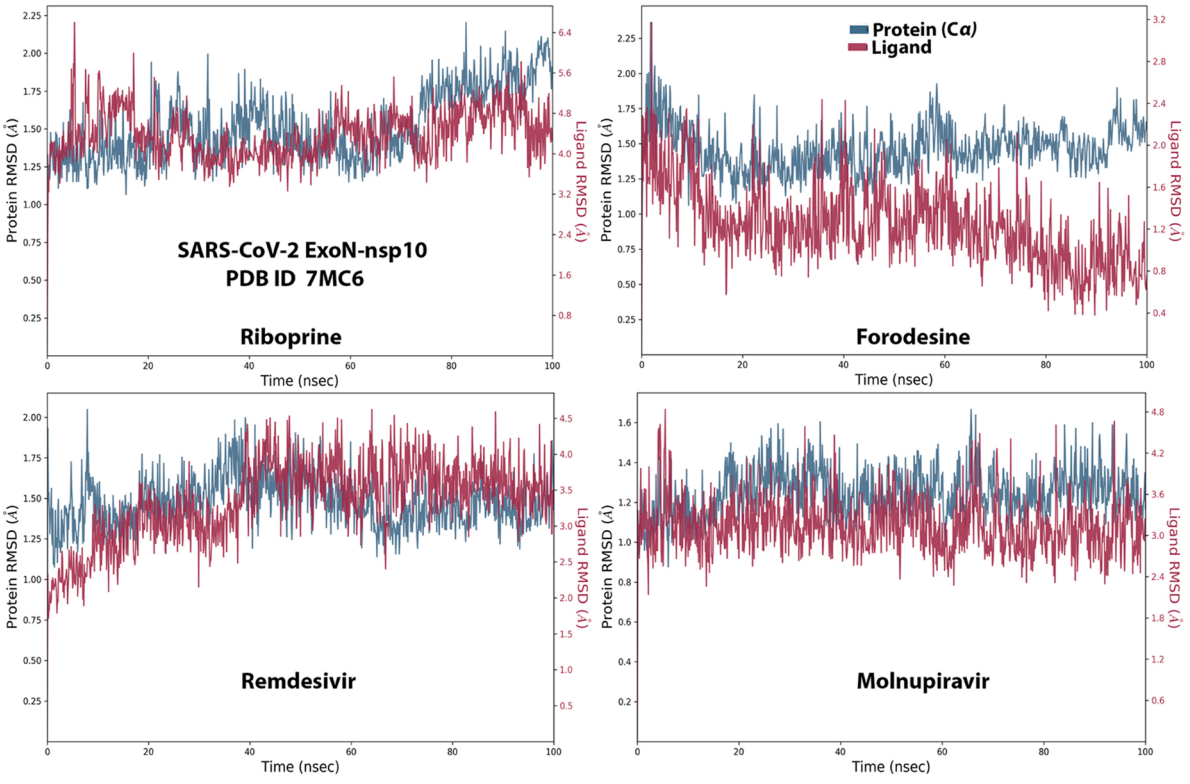

B

Fig. 2. RMSD trajectories (during a simulation period of 100 ns) of the α-carbon of amino acid residues of the protein (blue color) and the ligand (maroon color) in the protein-ligand complexes of the two NAs, riboprine and forodesine, and the two reference drugs, remdesivir and molnupiravir, respectively, with: (**A**) SARS-CoV-2 RdRp "nsp12" enzyme cocrystallized with its protein cofactors nsp7 and nsp8 (PDB ID: 7BV2). (**B**) SARS-CoV-2 ExoN "nsp14" enzyme cocrystallized with its protein cofactor nsp10 (PDB ID: 7MC6). For interpretation of the references to color in this figure legend, the reader is referred to the web version of this article.

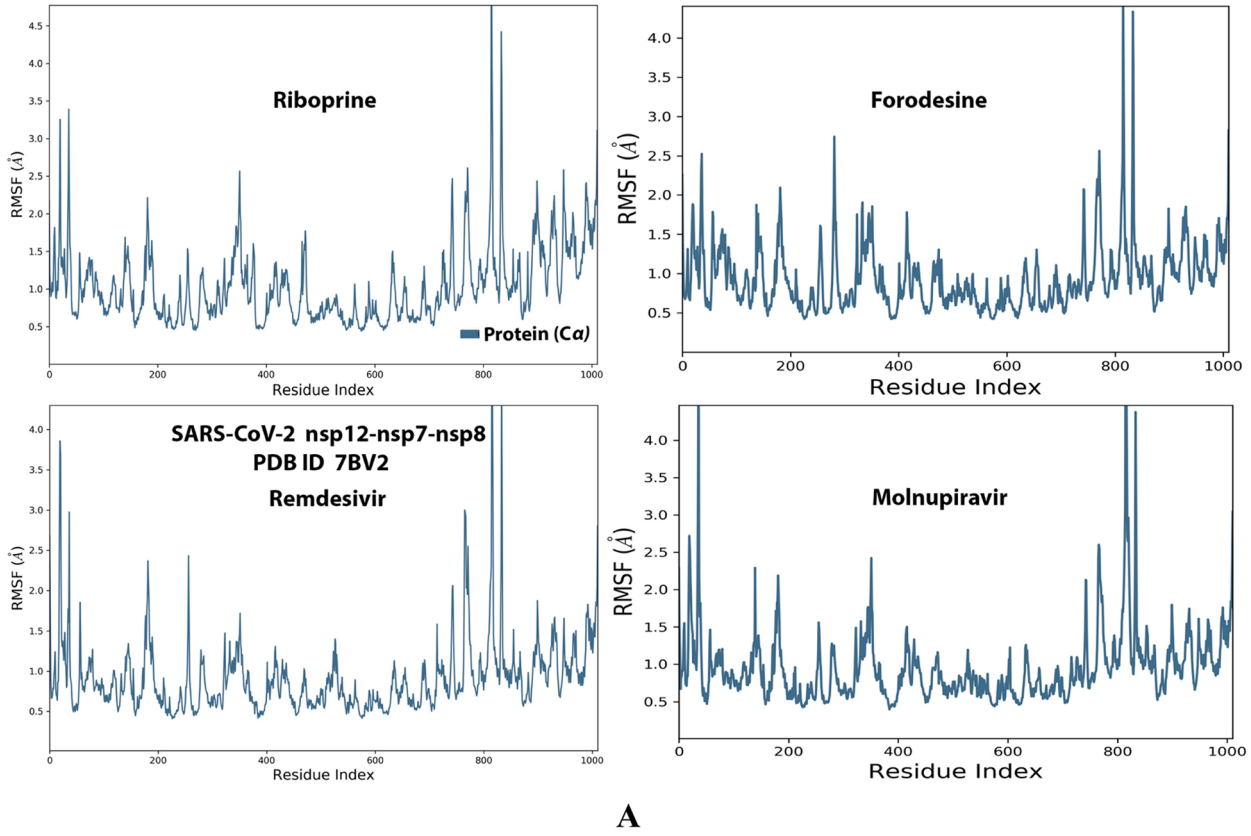

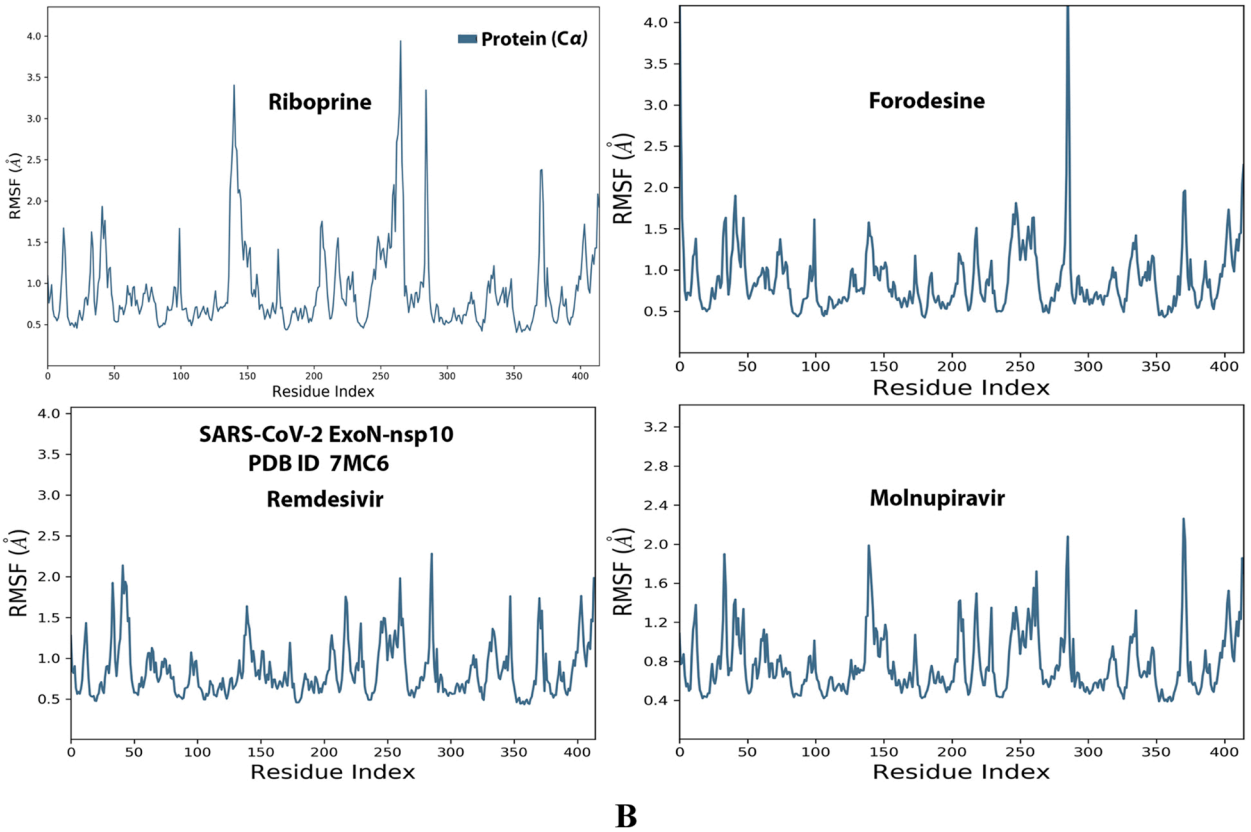

Fig. 3. RMSF trajectories (along the different residue regions) of the α-carbon of amino acid residues of the protein in the protein-ligand complexes of the two NAs, riboprine and forodesine, and the two reference drugs, remdesivir and molnupiravir, respectively, with: (**A**) SARS-CoV-2 RdRp "nsp12" enzyme cocrystallized with its protein cofactors nsp7 and nsp8 (PDB ID: 7BV2). (**B**) SARS-CoV-2 ExoN "nsp14" enzyme cocrystallized with its protein cofactor nsp10 (PDB ID: 7MC6).

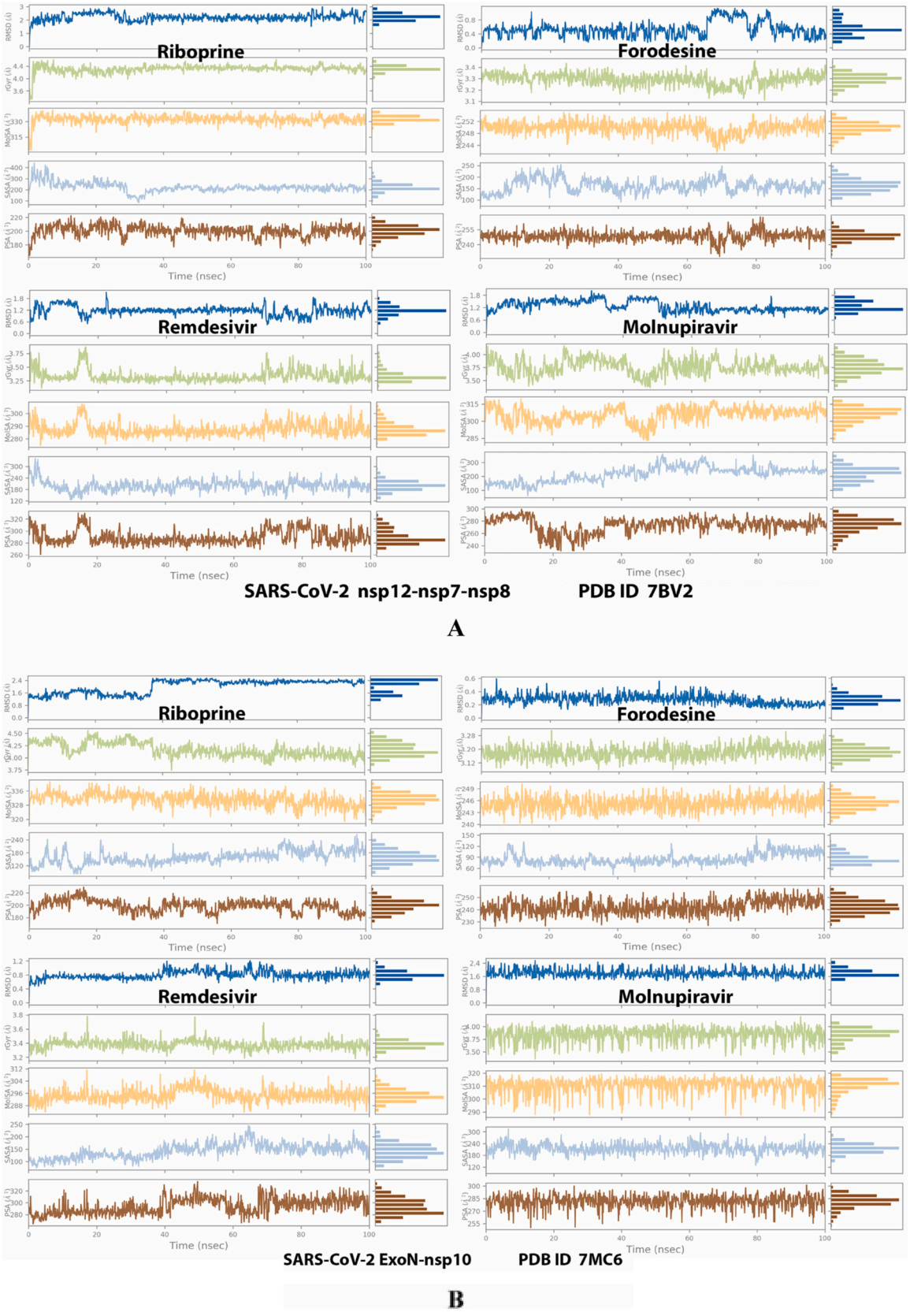

Fig. 4. Collective post-MD simulation analysis of the protein-ligand complexes properties (RMSD, rGyr, MolSA, SASA, and PSA) of the two NAs, riboprine and forodesine, and the two reference drugs, remdesivir and molnupiravir, respectively, with: (**A**) SARS-CoV-2 RdRp "nsp12" enzyme cocrystallized with its protein cofactors nsp7 and nsp8 (PDB ID: 7BV2). (**B**) SARS-CoV-2 ExoN "nsp14" enzyme cocrystallized with its protein cofactor nsp10 (PDB ID: 7MC6).

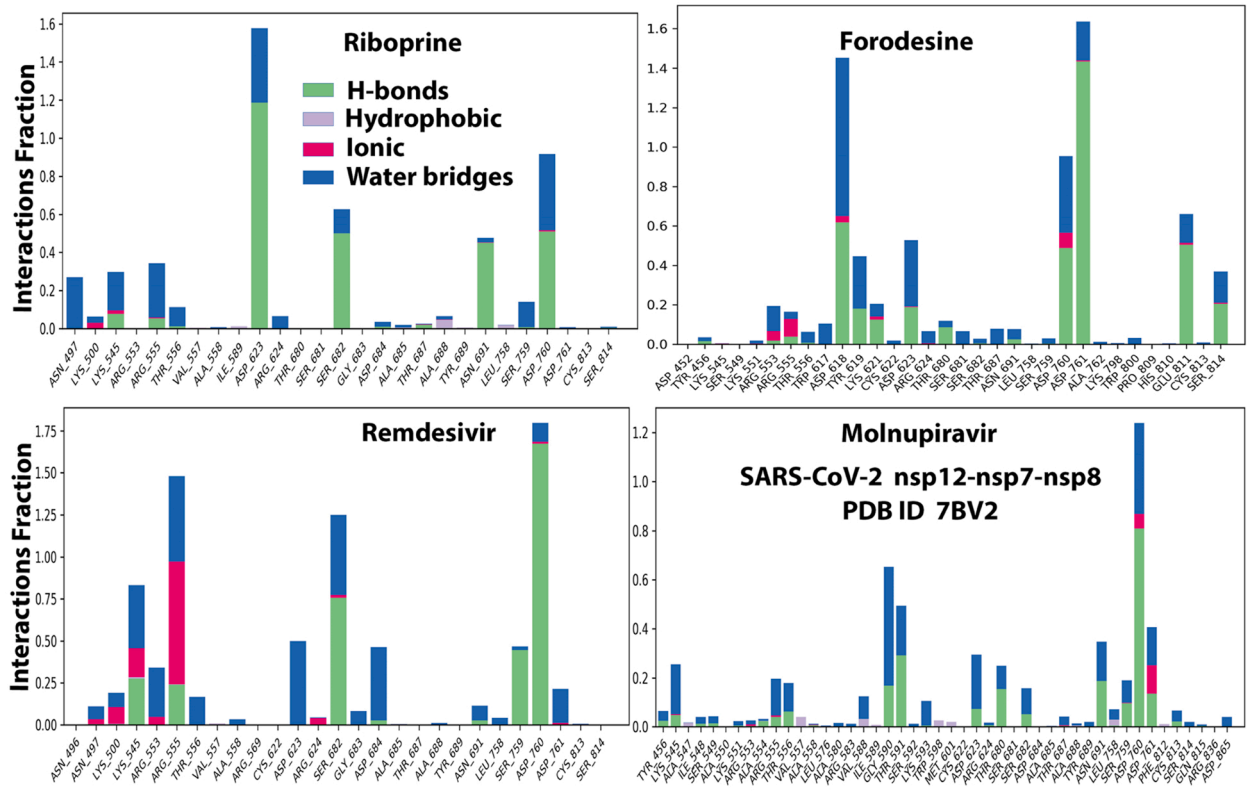

A

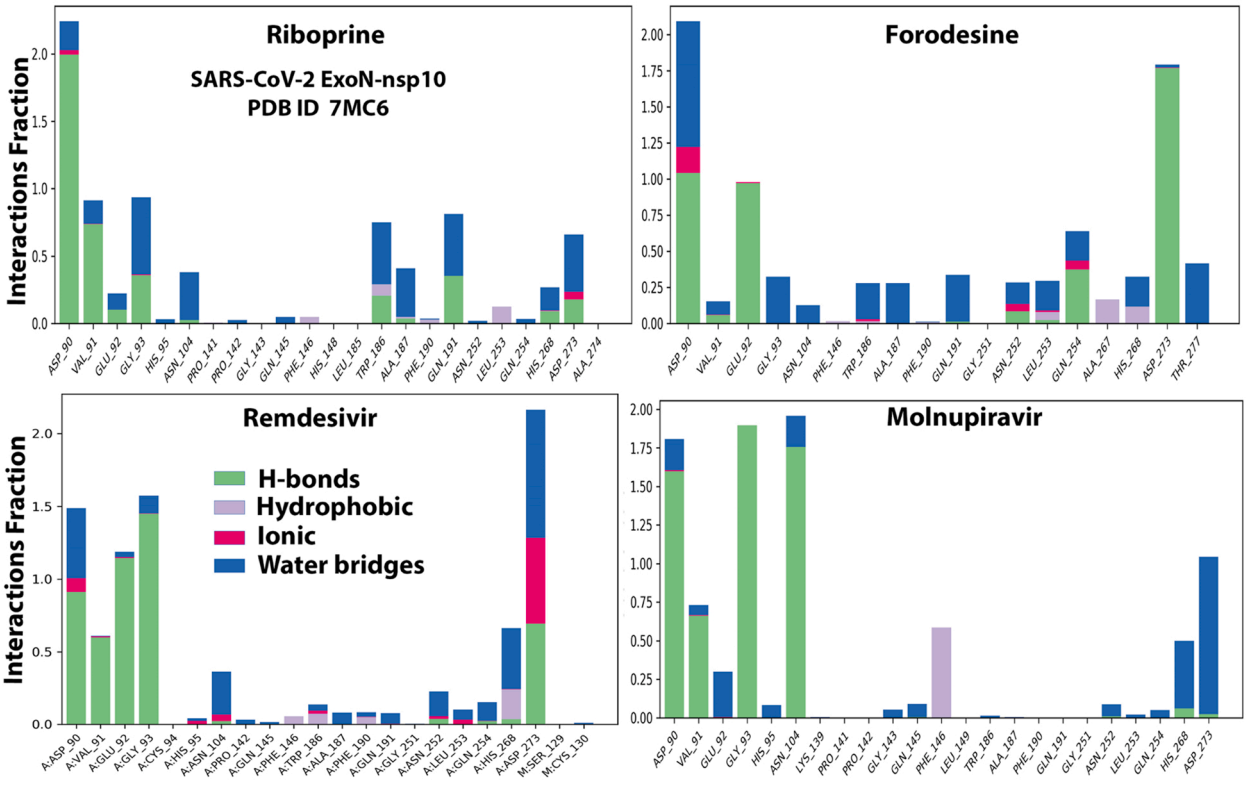

B

Fig. 5. Histograms of the protein-ligand interactions fractions throughout the simulative interaction trajectories of the two NAs, riboprine and forodesine, and the two reference drugs, remdesivir and molnupiravir, respectively, with: (**A**) SARS-CoV-2 RdRp "nsp12" enzyme cocrystallized with its protein cofactors nsp7 and nsp8 (PDB ID: 7BV2). (**B**) SARS-CoV-2 ExoN "nsp14" enzyme cocrystallized with its protein cofactor nsp10 (PDB ID: 7MC6).

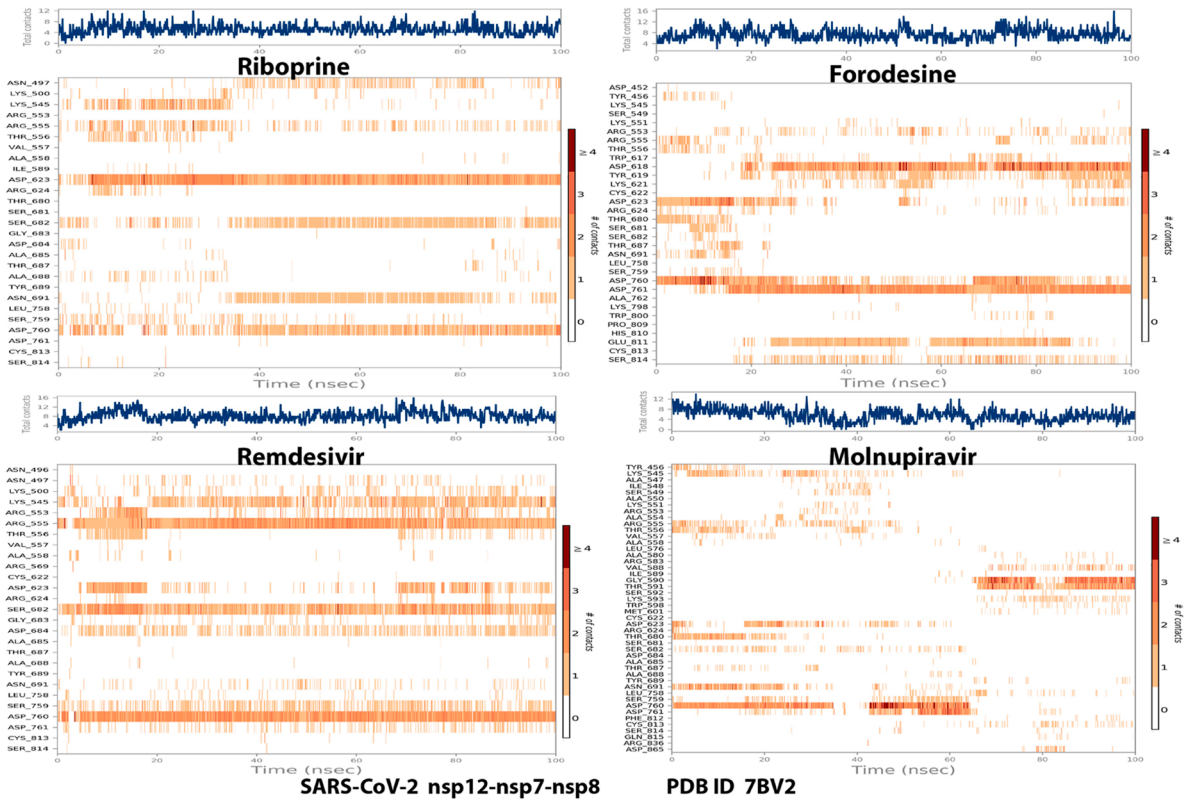

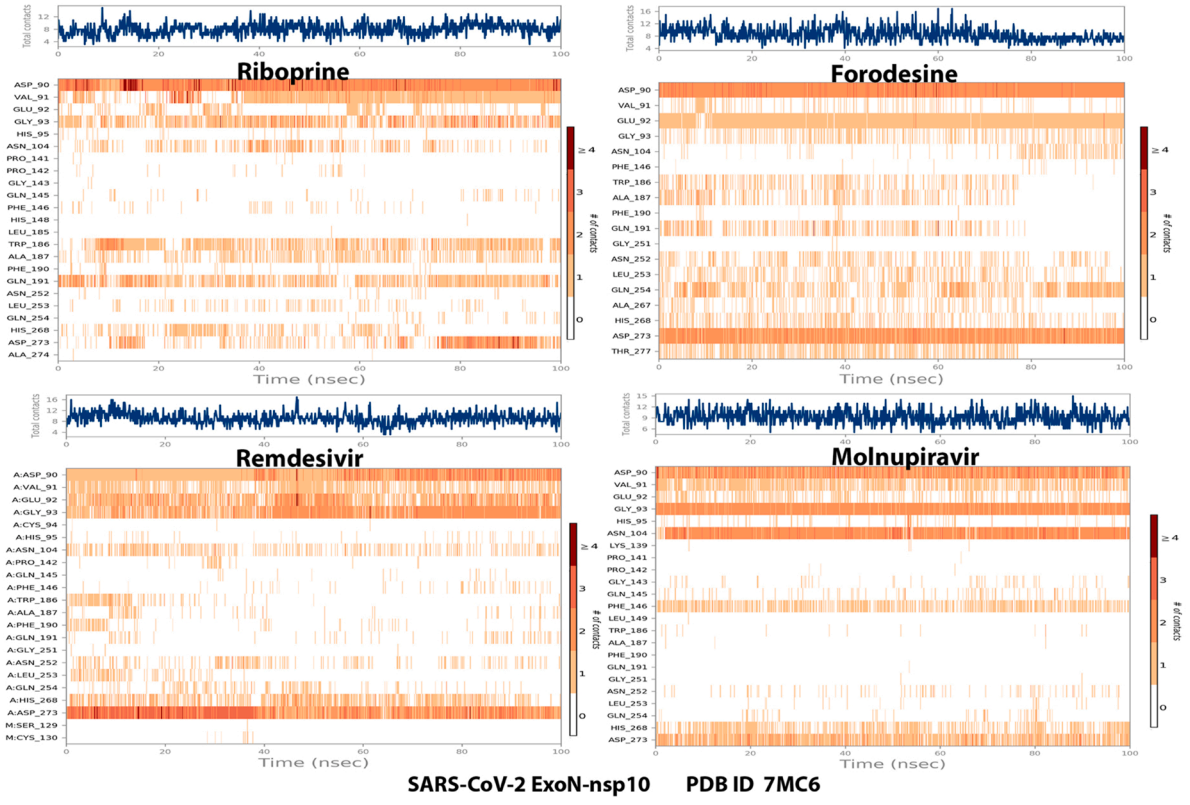

Fig. 6. Plots of the distribution of the total number of interactions (contacts) in each trajectory framework of the protein-ligand complexes of the two NAs, riboprine and forodesine, and the two reference drugs, remdesivir and molnupiravir, respectively, with: (**A**) SARS-CoV-2 RdRp "nsp12" enzyme cocrystallized with its protein cofactors nsp7 and nsp8 (PDB ID: 7BV2). (**B**) SARS-CoV-2 ExoN "nsp14" enzyme cocrystallized with its protein cofactor nsp10 (PDB ID: 7MC6).

interactions, ionic bonds, and water bridges (weaker in some examples), of relatively short bond distances and low binding energies.

Fig. S1, Fig. S2, Fig. S3, and Fig. S4, in the Supplementary Material file, show the elaborate 2D and 3D representations of the most apparent noncovalent interactions between each ligand of the six top ranked NAs (and also of the two reference drugs) with each of the two coronaviral-2 enzymes, respectively. The 3D representations focus mostly on the shortest bonds. The molecules of the six screened NAs strongly strike most of the neighboring active residues of the major active catalytic pockets of the two SARS-CoV-2 enzymes, RdRp and ExoN. The overall data of all noncovalent bond interactions were collected from the 2D, 3D, and MD simulations, as briefed in Table 1. These interactions are very favorable and very comparable to, or even in some cases more promising than, those of remdesivir/molnupiravir with the same two proteinous enzymes.

Analysis of the MD simulation results revealed the relatively good stabilities of the formed protein-ligand complexes of each of the six NAs with each of the two enzymes when compared with the reference drugs. Complexes of the NAs with SARS-CoV-2 ExoN are slightly more stable, with less numbers/intensities of fluctuations, and with lower RMSD (Å) and RMSF (Å) values than those with SARS-CoV-2 RdRp. Interestingly, riboprine and forodesine displayed the best results among all in most of the compared MD items during the simulation. Comprehensively, the RdRp-riboprine, RdRp-forodesine, ExoN-riboprine, and ExoN-forodesine complexes appear to be reasonably stable. The early fluctuations (which were not mostly extreme) in RMSF and RMSD trajectories may be indications of some conformational changes within the enzyme complex system as a result of the adequate repositioning of both ligands inside the catalytic binding sites which takes some nanotime till the formation of convenient and advantageous strong molecular interactions. Possible unrevealed allosteric modulations, specially in case of the larger protein complex SARS-CoV-2 nsp12-nsp7-nsp8, could also be put into consideration. Forodesine has the lowest rGyr values (less than 3.5 Å), among all the tested compounds including the reference ones, with both enzymes, indicating more compact and stable protein systems. In addition, from the computational point of view, forodesine followed by riboprine have the best balanced MolSA, SASA, and PSA values among all the investigated compounds. Interestingly, riboprine displayed the largest interactions fraction (of more than 2% of the total interactions predicted) of the strong H-bonds with the hit SARS-CoV-2 proteins, among all the tested compounds, and this occurs specifically with the catalytic amino acid residue Asp90 in the small protein SARS-CoV-2 nsp14-nsp10 in its relatively stable complex with riboprine, indicating a significant potential of riboprine to give a strongly-inhibited/blocked status of the ExoN enzyme. MD simulation results also confirmed nearly all the primary molecular docking data with regard to, for example, the interacting amino acids along with the numbers/types/strengths of the formed bonds. Fig. 2A,B, Fig. 3A,B, Fig. 4A,B, Fig. 5A,B, and Fig. 6A,B show the detailed results of MD simulation of the interactions between each ligand of the most promising NAs, riboprine and forodesine, with each of the two coronaviral-2 enzymes, RdRp and ExoN, respectively (in comparison with the two reference FDA-approved anti-SARS-CoV-2 RdRp drugs, remdesivir and molnupiravir). Table 2 summarizes the findings of Fig. 3A,B and Fig. 4A,B. The previous computational data were very encouraging to motivate us to transfer to the biological evaluation part of the current work.

3.2. *Experimental biological evaluation of the selected NAs as potential anti-COVID-19 drugs*

The first preclinical assay in this extensive assessment is the robust cell-based test, the *in vitro* anti-SARS-CoV-2 RdRp bioassay, which was recently developed using Gaussia-luciferase (Gluc) as the reporter to assess the anticoronaviral-2 RdRp activity of mainly NAs (the prodrugs or parent drugs of nucleotides) with no need for preparing the active nucleotidic triphosphate forms of the NAs (or of the other non-triphosphorylated nucleotidic analogs, *i.e.*, of the monophosphorylated and diphosphorylated NAs) as for the cell-free assays (Zhao et al., 2022, 2021). Moreover, it was obviously confirmed, through the outcomes of this new biochemical assay, that the exonuclease activity of SARS-CoV-2 nsp14 significantly improves the SARS-CoV-2 RdRp resistance to the various inhibitors of the nucleoside/nucleotide analogs class (one of the primary factors that aggravates the resistance and severe pathogenicity of SARS-CoV-2 particles is their abilities to encode the nsp14 ExoN which is capable of taking off the faulty mutagenic nucleotides mis-incorporated by the low-fidelity RdRp into the growing coronaviral-2 RNA strands, bringing about considerable resistance to nucleos(t)ide analog therapeutic agents), thus ExoN effects were considered and added in the steps of this evaluation assay protocol which was primarily designed for exploring possible SARS-CoV-2 RdRp inhibitors (dissimilar to the traditional analytical cell-free assay) (Zhao et al., 2022, 2021; Smith et al., 2013; Ferron et al., 2018). The assay can be metaphorically called "anti-SARS-CoV-2 RdRp/ExoN bioassay".

As formerly mentioned, we principally concentrate in the current study on the two principal protein complexes that catalyze and control the SARS-CoV-2 replication/transcription processes, nsp12-nsp7-nsp8 polymerase complex and nsp14-nsp10 exoribonuclease complex, respectively. This test significantly imitates the respective original replication processes that occur for the SARS-CoV-2 genome, as it practically simulates the RNA generating pathways driven mainly by the SARS-CoV-2 RdRp (Hillen et al., 2020). Table 3 displays the detailed values obtained from this *in vitro* anti-SARS-CoV-2 RdRp/ExoN bioassay. The resultant data showed that, among the tested target NAs, riboprine and forodesine displayed the best results. The two compounds effectively inhibited SARS-CoV-2 RdRp activity with very excellent small EC_{50} values of 189 and 207 nM, which very slightly increased in the presence of SARS-CoV-2 ExoN (the wild type) to about 288 and 317 nM, respectively, indicating the potent inhibitory/blocking activities of both drugs against SARS-CoV-2 ExoN, which appeared in these very small nanomolar differences of the EC_{50} values between the two cases. Mutations in the exoribonuclease (*i.e.*, the mutated ExoN type; *e.g.*, D90A/E92A mutations of the major active catalytic site in nsp14 as in our current case) reinforced the anti-RdRp potency of riboprine and forodesine to excellent EC_{50} values of 235 and 260 nM (*i.e.*, slightly lower than that resulted in the presence of the normal wild type of ExoN; these very slight changes also reflected, as previously mentioned, the powerful activities of both NAs against SARS-CoV-2 ExoN in its original wild type from the beginning prior to any intended mutations). These previous values of riboprine and forodesine even surpassed those of the two potent reference agents, remdesivir and molnupiravir, reflecting the

Table 2
A summary of some important MD simulation parameters, estimated in the current study, of the top ranked NAs riboprine and forodesine (using remdesivir and molnupiravir as the positive control drugs) upon a 100-ns docking/interaction run with RdRp (7BV2) and ExoN (7MC6) proteins, respectively.

Classification	Compound Name	MD Simulation Parameters *(most prominent and stable values in the productive regions; with RdRp (7BV2)/ExoN (7MC6))*					
		RMSD (Å)	RMSF (Å)	rGyr (Å)	MolSA (Å^2)	SASA (Å^2)	PSA (Å^2)
Top Ranked NAs	**Riboprine**	**1.7/1.3**	**< 2.5/< 0.2**	**4.3/4.0**	**330/328**	**200/180**	**200/200**
	Forodesine	**0.4/0.2**	**< 2.0/< 2.0**	**3.3/3.2**	**250/246**	**150/90**	**255/240**
Positive Control Drugs	**Remdesivir**	**1.1/0.8**	**< 3.0/< 2.5**	**3.3/3.4**	**290/300**	**240/200**	**295/320**
	Molnupiravir	**0.8/1.7**	**< 2.5/< 2.5**	**3.9/4.0**	**315/320**	**250/240**	**285/295**

Table 3
Anti-SARS-CoV-2 RdRp/ExoN activities (along with respective ratios) of the target repurposed drugs riboprine, forodesine, nelarabine, tecadenoson, maribavir, and vidarabine (using both remdesivir and molnupiravir as the positive control/reference drugs, and DMSO as the negative control/placebo drug), respectively, in HEK293T cells, expressed as EC_{50} values in nM (please note that, in this table, nsp12 refers to nsp12/7/8 complex, nsp14 refers to nsp14/10 complex, and $nsp14_{mutant}$ refers to $nsp14_{mutant}$/10 complex).

Classification	Compound Name	Inhibition of SARS-CoV-2 RdRp *in vitro* (EC_{50} in nM)[a]			Respective Ratios of EC_{50}	
		Nsp12	Nsp12 + Nsp14	Nsp12 + $Nsp14_{mutant}$	(Nsp12 + Nsp14)/Nsp12	(Nsp12 + $Nsp14_{mutant}$)/Nsp12
Repurposed NAs	**Riboprine**	**189 ± 20**	**288 ± 31**	**235 ± 24**	**1.52**	**1.24**
	Forodesine	**207 ± 23**	**317 ± 34**	**260 ± 29**	**1.53**	**1.26**
	Nelarabine	**644 ± 41**	**1234 ± 65**	**1097 ± 53**	**1.92**	**1.70**
	Tecadenoson	**981 ± 59**	**1355 ± 63**	**1300 ± 60**	**1.38**	**1.33**
	Maribavir	**1056 ± 54**	**1891 ± 69**	**1458 ± 66**	**1.79**	**1.38**
	Vidarabine	**1077 ± 51**	**2031 ± 75**	**1500 ± 68**	**1.89**	**1.39**
Reference Drugs	**Remdesivir**	**1128 ± 62**	**2124 ± 81**	**1562 ± 69**	**1.88**	**1.39**
	Molnupiravir	**251 ± 29**	**448 ± 42**	**325 ± 37**	**1.79**	**1.30**
Placebo Solvent	**DMSO**	**> 100000**	**> 100000**	**> 100000**	**N.A.[b]**	**N.A.**

[a] EC_{50} or 50% effective concentration is the concentration of the tested compound that is required for 50% reduction in the COVID-19 polymerase (SARS-CoV-2 RdRp) activity *in vitro*. EC_{50} is expressed in nM.
[b] N.A. means not available (*i.e.*, it was not determined).

Table 4
Anti-SARS-CoV-2/anti-COVID-19 activities (along with cytotoxicities) of the target repurposed drugs riboprine, forodesine, nelarabine, tecadenoson, maribavir, and vidarabine (using both remdesivir and molnupiravir as the positive control/reference drugs, and DMSO as the negative control/placebo drug), respectively, against SARS-CoV-2 (Omicron variant, B.1.1.529/BA.5 sublineage) in Vero E6 cells.

Classification	Compound Name	CC_{50}[a] (nM)	Inhibition of SARS-CoV-2 Replication *in vitro* (Anti-B.1.1.529/BA.5 Bioactivities) (nM)			
			100% CPE Inhibitory Concentration ($CPEIC_{100}$)[b]	50% Reduction in Infectious Virus (EC_{50})[c]	50% Reduction in Viral RNA Copy (EC_{50})[d]	90% Reduction in Infectious Virus (EC_{90})[e]
Repurposed NAs	**Riboprine**	**> 100000**	**1110 ± 47**	**408 ± 22**	**428 ± 24**	**1590 ± 61**
	Forodesine	**> 100000**	**1600 ± 65**	**657 ± 34**	**688 ± 41**	**1997 ± 69**
	Nelarabine	**> 100000**	**4105 ± 149**	**1656 ± 71**	**1744 ± 73**	**6335 ± 186**
	Tecadenoson	**> 100000**	**7645 ± 240**	**2799 ± 109**	**2929 ± 117**	**11876 ± 298**
	Maribavir	**> 100000**	**7986 ± 277**	**3000 ± 131**	**3102 ± 143**	**12198 ± 327**
	Vidarabine	**> 100000**	**8042 ± 288**	**3190 ± 130**	**3246 ± 145**	**12621 ± 352**
Reference Drugs	**Remdesivir**	**> 100000**	**5883 ± 255**	**2003 ± 87**	**2062 ± 95**	**7960 ± 281**
	Molnupiravir	**> 100000**	**6190 ± 275**	**2579 ± 105**	**2665 ± 107**	**9101 ± 293**
Placebo Solvent	**DMSO**	**> 100000**	**> 100000**	**> 100000**	**> 100000**	**> 100000**

[a] CC_{50} or 50% cytotoxic concentration is the concentration of the tested compound that kills half the cells in an uninfected cell culture. CC_{50} was determined with serially-diluted compounds in Vero E6 cells at 48 h postincubation using CellTiter-Glo Luminescent Cell Viability Assay (Promega).
[b] $CPEIC_{100}$ or 100% CPE inhibitory concentration is the lowest concentration of the tested compound that causes 100% inhibition of the cytopathic effects (CPE) of SARS-CoV-2 B.1.1.529/BA.5 virus in Vero E6 cells under increasing concentrations of the tested compound at 48 h postinfection. Compounds were serially diluted from 100,000 nM concentration.
[c] EC_{50} or 50% effective concentration is the concentration of the tested compound that is required for 50% reduction in infectious SARS-CoV-2 B.1.1.529/BA.5 virus particles *in vitro*. EC_{50} is determined by infectious virus yield in culture supernatant at 48 h postinfection (log_{10} $TCID_{50}$/mL).
[d] EC_{50} or 50% effective concentration is the concentration of the tested compound that is required for 50% reduction in SARS-CoV-2 B.1.1.529/BA.5 viral RNA copies *in vitro*. EC_{50} is determined by viral RNA copies number in culture supernatant at 48 h postinfection (log_{10} RNA copies/mL).
[e] EC_{90} or 90% effective concentration is the concentration of the tested compound that is required for 90% reduction in infectious SARS-CoV-2 B.1.1.529/BA.5 virus particles *in vitro*. EC_{90} is determined by infectious virus yield in culture supernatant at 48 h postinfection (log_{10} $TCID_{90}$/mL).

possible superiority of both NAs over remdesivir/molnupiravir in clinical investigation in humans. The results also proved that molnupiravir and remdesivir could not resist the performance of Omicron variant ExoN the same way/potency riboprine and forodesine could do. The other target NAs (nelarabine, tecadenoson, maribavir, and vidarabine) also showed very good promising small values, but with less degree than those of riboprine, forodesine, and the reference molnupiravir, respectively. It is apparently observed from the values in Table 3 that as much the EC_{50} values of the NA against the polymerase alone and against the polymerase in the presence of the exoribonuclease are close to each other, as more potent this NA inhibitor is (*i.e.*, as more predicted for this examined NA to be an ideally effective RdRp inhibitor or, more precisely, an ideally effective SARS-CoV-2 replication inhibitor). From the results we can also conclude that an ideal potent SARS-CoV-2 RdRp inhibitor should have a ratio of $EC_{50(polymerase\ +\ exoribonuclease)}/EC_{50(polymerase)}$ that is very close to 1 and less than 2. As this ratio decreases, as the compound has higher potentials to succeed in inhibiting the SARS-CoV-2 replication more perfectly. Riboprine displayed the highest resistance, among all the tested compounds, to the coronaviral-2 nsp14 exoribonuclease activity in HEK293T cells. The very promising capabilities of riboprine and forodesine to inhibit the nsp12 polymerase and nsp14 exoribonuclease activities of the coronaviral-2 Omicron variant interestingly uphold the repurposing potentials of riboprine and forodesine in clinical settings for further therapeutic use as potent anti-COVID-19 drugs. It is worth mentioning that riboprine and forodesine are nearly the only NAs that have such unique potent anti-SARS-CoV-2 activities against both the RdRp and ExoN enzymes of the newest SARS-CoV-2 variant, the Omicron variant, in very significant values to date (this is to the best of our current knowledge during the submission of this research paper for publication) (Zhao et al., 2022, 2021). These present biochemical findings concerning the potent inhibitory SARS-CoV-2 RdRp-binding and ExoN-binding properties of riboprine and forodesine are in an ideal agreement with almost all the computed parameters of the prior *in silico* part of this comprehensive research, which was discussed in details in Subsection 3.1.

The second assay is the collective *in vitro* anti-SARS-CoV-2 and

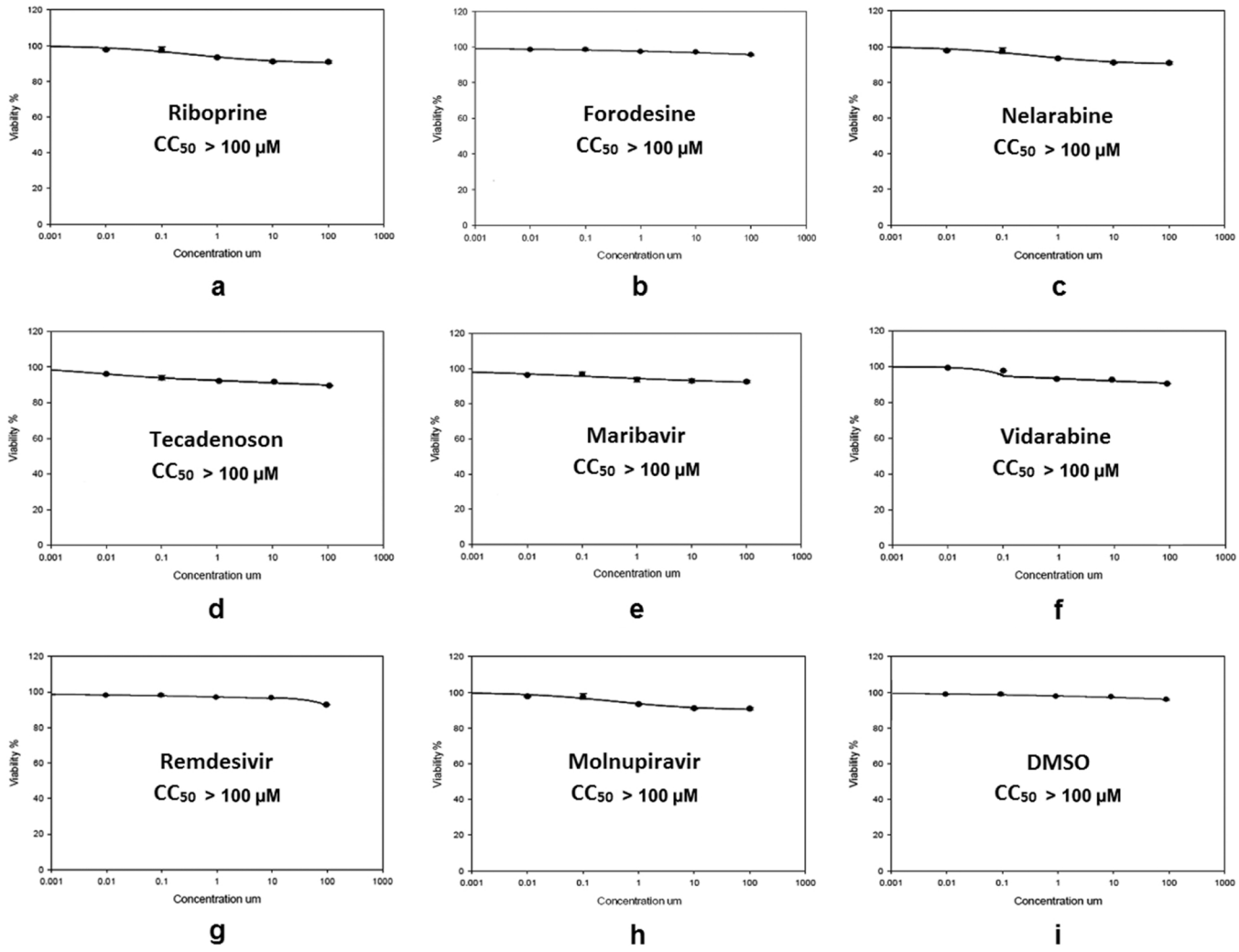

Fig. 7. Cytotoxicity graphs obtained in the current study for: (**a**) Riboprine, (**b**) Forodesine, (**c**) Nelarabine, (**d**) Tecadenoson, (**e**) Maribavir, (**f**) Vidarabine, (**g**) Remdesivir, (**h**) Molnupiravir, and (**i**) DMSO.

cytotoxicity tests. Table 4 shows the resultant values from both tests in details. The used SARS-CoV-2 strain in the anticoronaviral-2 assay is the new variant of SARS-CoV-2, the Omicron variant B.1.1.529/BA.5 sublineage, which is the newest infectious and resistant substrain of the virus. The data presented in Table 4 interestingly disclosed the considerably higher antiviral efficacies of riboprine and forodesine on the recently-appeared variants/subvariants of SARS-CoV-2 as compared to those of remdesivir and molnupiravir (DMSO displayed extremely little effects, *i.e.*, negligible findings). Riboprine and forodesine were found to efficiently inhibit and deactivate the entire SARS-CoV-2 replication/transcription process in Vero E6 cells with EC_{50} values extremely smaller than the 100,000 nM value of the stock concentration, continuing their superiorities over the other evaluated target NAs exactly as in the previous anti-RdRp/ExoN biochemical assay. Promisingly, the natural NA riboprine was found to be very leading (*i.e.*, ranked first among all the tested compounds) in its total anti-Omicron activity (EC_{50} = 408 nM), which was found to be about 4.9 and 6.3 times as potent as the two reference drugs, remdesivir (EC_{50} = 2003 nM) and molnupiravir (EC_{50} = 2579 nM), respectively, with respect to the tested *in vitro* anti-B.1.1.529/BA.5/anti-SARS-CoV-2 activity. Whilst forodesine was ranked second, among all the assayed compounds, in its total anti-Omicron activity (EC_{50} = 657 nM), which was found to be about 3.1 and 3.9 times as active as the two reference drugs, remdesivir and molnupiravir, respectively, with respect to the same estimated activity. According to the present cytotoxicity assay, the *in vitro* CC_{50} values of riboprine and forodesine are significantly greater than 100,000 nm or 100 μM, therefore these two compounds are expected to have advantageous high corresponding clinical selectivity indices "SIs" ($SI_{riboprine} > 245.1$ and $SI_{forodesine} > 152.2$; while remdesivir and molnupiravir have narrower SIs, $SI_{remdesivir} > 49.9$ and $SI_{molnupiravir} > 38.8$), suggesting the selective anti-RNA actions of the riboprine and forodesine molecules against the new coronaviral-2 Omicron genome rather than the human genome. Fig. 7 demonstrates the cytotoxicity graphs of all the examined NAs and their controls from the anti-SARS-CoV-2 test. Riboprine and forodesine displayed significantly small values of the concentration that results in 100% *in vitro* inhibition of the coronaviral-2 Omicron variant cytopathic effects ($CPEIC_{100}$ = 1110 and 1600 nM, respectively), which are less than the corresponding values of remdesivir ($CPEIC_{100}$ = 5883 nM) and molnupiravir ($CPEIC_{100}$ = 6190 nM) and also less than those of the other tested NAs. In line with their potent activities against the infectious coronaviral-2 B.1.1.529/BA.5 substrain, riboprine and forodesine also showed very slight values of the concentration that is required for 50% *in vitro* lowering in the number of RNA copies of the B.1.1.529/BA.5 substrain of SARS-CoV-2 (428 and 688 nM, respectively), which are obviously smaller than the corresponding values of both remdesivir and molnupiravir (2062 and 2665 nM, respectively). EC_{90} values for riboprine and forodesine, which are preferably used for the *in vivo*/clinical studies, were also very small and compliant with the EC_{50} values (being not far that much from the EC_{50} values indicates the expected significant clinical potencies of both drugs) as demonstrated in

Table 4. Nelarabine, tecadenoson, maribavir, and vidarabine showed slightly higher concentration values (EC_{50}, EC_{90}, CC_{50}, and $CPEIC_{100}$) than those showed by riboprine and forodesine, but still comparable to those of the positive control drugs, remdesivir and molnupiravir.

It was surprisingly noted that riboprine and forodesine successfully act against the SARS-CoV-2 particles in a relatively quick mode of action, with their utmost effectiveness against the Omicron variant reached during 3.5–9.5 h of administration/treatment starter. Quite as their natural analogs, the triphosphate forms of riboprine and forodesine (riboprine-TP and forodesine-TP), which are pharmacokinetically recognized as the major metabolic phosphorylated esters of the two drugs, are expected to be as active as the administered original forms or even much more (due to higher biocompatibility). Lately, few studies reported similar favorable findings of some NAs but on other subvariants of the SARS-CoV-2 Omicron variant (Rabie and Abdalla, 2023). The present results of this reliable bioassay are in an excellent agreement with almost all the outcomes of the above-discussed anti-RdRp biochemical assay and computational study of the current comprehensive research.

4. Conclusions and prospective medicinal applications

Recently, nucleoside antivirals/antimicrobials topped the scene as significantly effective choices for COVID-19 treatment (Jockusch et al., 2020). The current inclusive *in silico/in vitro* preclinical study disclosed the anti-SARS-CoV-2 potentials of a series of NAs, with riboprine and forodesine being the most promising potent SARS-CoV-2 RNA mutagens or, at least, the most promising coronaviral-2 replication inhibitors in general. Riboprine is a natural purine NA (mainly a plant metabolite), previously examined for some important various pharmacological actions, *e.g.*, antineoplastic, proapoptotic, neuroprotective, and anti-angiogenic activities (PubChem, 2022), whereas forodesine is a very potent synthetic and unique highly selective transition-state analog inhibitor of purine nucleoside phosphorylase (PNP), approved and used recently for the efficient treatment of refractory/relapsed peripheral T-cell lymphoma (Kicska et al., 2001). From the physical point of view, riboprine and forodesine molecules have considerably pliable chemical structures that can easily tolerate chemical modifications in biosystems. It was clearly revealed in the current research work that coronaviral-2 microparticles are very sensitive to both drugs and thoroughly mutated and inhibited by them. Interestingly, it was found that riboprine and forodesine may effectively prevent SARS-CoV-2 spreadability and pathogenicity (and, accordingly, terminate COVID-19 infection as a whole) in the human body, mainly through severely blocking the SARS-CoV-2 replication *via* a double synergistic inhibitory mode of action against the two vital SARS-CoV-2 enzymes, RdRp/ExoN. This double mode of anticoronaviral action could be extended to a triple one if the anticipated inhibitory effects of the two agents against kinases, specially on ADK, are extensively explored and confirmed in a subsequent study. Similar to their natural analogs, the triphosphate esters of riboprine and forodesine are predicted to be as effective as the administered prodrugs. Based on the present research observations and results, the two NAs, riboprine and forodesine, should be specifically given high priority for development as prospective anti-COVID-19 remedies (with very encouraging anti-SARS-CoV-2 EC_{50} values of 408 and 657 nM, respectively, against the SARS-CoV-2 B.1.1.529/BA.5 subvariant), whereas all the six promising explored NAs (riboprine, forodesine, nelarabine, tecadenoson, maribavir, and vidarabine, respectively) generally require vast pharmacological and clinical studies to well understand their exact therapeutic values as candidate anti-SARS-CoV-2 drugs.

Declaration of Competing Interest

The authors declare that they have no known competing financial interests or personal relationships that could have appeared to influence the work reported in this paper.

Acknowledgments

This new discovery did not receive any external funding. The authors gratefully thank anyone who helped to make this new discovery and work coming out to light.

Appendix A. Supporting information

Supplementary data associated with this article can be found in the Supplementary Material file of the online version at doi:10.1016/j.compbiolchem.2022.107768.

References

Brunotte, L., Zheng, S., Mecate-Zambrano, A., Tang, J., Ludwig, S., Rescher, U., Schloer, S., 2021. Combination Therapy with Fluoxetine and the Nucleoside Analog GS-441524 Exerts Synergistic Antiviral Effects against Different SARS-CoV-2 Variants In Vitro. Pharmaceutics 13 (9), 1400. https://doi.org/10.3390/pharmaceutics13091400.

Cai, Q., Yang, M., Liu, D., Chen, J., Shu, D., Xia, J., Liao, X., Gu, Y., Cai, Q., Yang, Y., Shen, C., Li, X., Peng, L., Huang, D., Zhang, J., Zhang, S., Wang, F., Liu, J., Chen, L., Chen, S., Wang, Z., Zhang, Z., Cao, R., Zhong, W., Liu, Y., Liu, L., 2020. Experimental Treatment with Favipiravir for COVID-19: An Open-Label Control Study. Engineering 6 (10), 1192–1198. https://doi.org/10.1016/j.eng.2020.03.007.

Chien, M., Anderson, T.K., Jockusch, S., Tao, C., Li, X., Kumar, S., Russo, J.J., Kirchdoerfer, R.N., Ju, J., 2020. Nucleotide Analogues as Inhibitors of SARS-CoV-2 Polymerase, a Key Drug Target for COVID-19. J. Proteome Res. 19 (11), 4690–4697. https://doi.org/10.1021/acs.jproteome.0c00392.

Chitalia, V.C., Munawar, A.H., 2020. A painful lesson from the COVID-19 pandemic: the need for broad-spectrum, host-directed antivirals. J. Transl. Med. 18 (1), 390. https://doi.org/10.1186/s12967-020-02476-9.

Doharey, P.K., Singh, V., Gedda, M.R., Sahoo, A.K., Varadwaj, P.K., Sharma, B., 2022. *In silico* study indicates antimalarials as direct inhibitors of SARS-CoV-2-RNA dependent RNA polymerase. J. Biomol. Struct. Dyn. 40 (12), 5588–5605. https://doi.org/10.1080/07391102.2021.1871956.

DrugDevCovid19. RdRp. Available from: ⟨http://clab.labshare.cn/covid/php/database_target.php?target=RdRp&id=P0DTD1⟩ (last Accessed 2 August 2022a).

DrugDevCovid19. Nsp14. Available from: ⟨http://clab.labshare.cn/covid/php/database_target.php?target=nsp14&id=P0DTD1⟩ (last Accessed 2 August 2022b).

Eissa, I.H., Khalifa, M.M., Elkaeed, E.B., Hafez, E.E., Alsfouk, A.A., Metwaly, A.M., 2021. *In Silico* Exploration of Potential Natural Inhibitors against SARS-Cov-2 nsp10. Molecules 26 (20), 6151. https://doi.org/10.3390/molecules26206151.

Ferron, F., Subissi, L., Silveira De Morais, A.T., Le, N.T.T., Sevajol, M., Gluais, L., Decroly, E., Vonrhein, C., Bricogne, G., Canard, B., Imbert, I., 2018. Structural and molecular basis of mismatch correction and ribavirin excision from coronavirus RNA. Proc. Natl. Acad. Sci. U. S. A. 115 (2), E162–E171. https://doi.org/10.1073/pnas.1718806115.

Hillen, H.S., Kokic, G., Farnung, L., Dienemann, C., Tegunov, D., Cramer, P., 2020. Structure of replicating SARS-CoV-2 polymerase. Nature 584 (7819), 154–156. https://doi.org/10.1038/s41586-020-2368-8.

Imran, M., Kumar Arora, M., Asdaq, S.M.B., Khan, S.A., Alaqel, S.I., Alshammari, M.K., Alshehri, M.M., Alshrari, A.S., Mateq Ali, A., Al-shammeri, A.M., Alhazmi, B.D., Harshan, A.A., Alam, M.T., Abida, 2021. Discovery, Development, and Patent Trends on Molnupiravir: A Prospective Oral Treatment for COVID-19. Molecules 26 (19), 5795. https://doi.org/10.3390/molecules26195795.

Ip, A., Ahn, J., Zhou, Y., Goy, A.H., Hansen, E., Pecora, A.L., Sinclaire, B.A., Bednarz, U., Marafelias, M., Sawczuk, I.S., Underwood III, J.P., Walker, D.M., Prasad, R., Sweeney, R.L., Ponce, M.G., La Capra, S., Cunningham, F.J., Calise, A.G., Pulver, B. L., Ruocco, D., Mojares, G.E., Eagan, M.P., Ziontz, K.L., Mastrokyriakos, P., Goldberg, S.L., 2021. Hydroxychloroquine in the treatment of outpatients with mildly symptomatic COVID-19: a multi-center observational study. BMC Infect. Dis. 21 (1), 72. https://doi.org/10.1186/s12879-021-05773-w.

Jockusch, S., Tao, C., Li, X., Anderson, T.K., Chien, M., Kumar, S., Russo, J.J., Kirchdoerfer, R.N., Ju, J., 2020. A library of nucleotide analogues terminate RNA synthesis catalyzed by polymerases of coronaviruses that cause SARS and COVID-19. Antiviral Res. 180, 104857. https://doi.org/10.1016/j.antiviral.2020.104857.

Kaur, H., Sarma, P., Bhattacharyya, A., Sharma, S., Chhimpa, N., Prajapat, M., Prakash, A., Kumar, S., Singh, A., Singh, R., Avti, P., Thota, P., Kumar, B., 2021. Efficacy and safety of dihydroorotate dehydrogenase (DHODH) inhibitors "leflunomide" and "teriflunomide" in Covid-19: a narrative review. Eur. J. Pharmacol. 906, 174233. https://doi.org/10.1016/j.ejphar.2021.174233.

Khater, S., Kumar, P., Dasgupta, N., Das, G., Ray, S., Prakash, A., 2021. Combining SARS-CoV-2 Proofreading Exonuclease and RNA-Dependent RNA Polymerase Inhibitors as a Strategy to Combat COVID-19: a High-Throughput *in silico* Screening. Front. Microbiol. 12, 647693. https://doi.org/10.3389/fmicb.2021.647693.

Kicska, G.A., Long, L., Hörig, H., Fairchild, C., Tyler, P.C., Furneaux, R.H., Schramm, V. L., Kaufman, H.L., 2001. Immucillin H, a powerful transition-state analog inhibitor of purine nucleoside phosphorylase, selectively inhibits human T lymphocytes. Proc.

Natl. Acad. Sci. U. S. A. 98 (8), 4593–4598. https://doi.org/10.1073/pnas.071050798.
Lin, X., Liang, C., Zou, L., Yin, Y., Wang, J., Chen, D., Lan, W., 2021. Advance of structural modification of nucleosides scaffold. Eur. J. Med. Chem. 214, 113233. https://doi.org/10.1016/j.ejmech.2021.113233.
Mahase, E., 2021. Covid-19: Pfizer's paxlovid is 89% effective in patients at risk of serious illness, company reports. BMJ 375, n2713. https://doi.org/10.1136/bmj.n2713.
Moeller, N.H., Shi, K., Demir, Ö., Belica, C., Banerjee, S., Yin, L., Durfee, C., Amaro, R.E., Aihara, H., 2022. Structure and dynamics of SARS-CoV-2 proofreading exoribonuclease ExoN. Proc. Natl. Acad. Sci. U. S. A. 119 (9), e2106379119. https://doi.org/10.1073/pnas.2106379119.
Moirangthem, D.S., Surbala, L., 2021. Remdesivir (GS-5734) in COVID-19 Therapy: The Fourth Chance. Curr. Drug Targets 22 (12), 1346–1356. https://doi.org/10.2174/1389450121999201202110303.
PubChem. Riboprine. PubChem CID: 24405, available from ⟨https://pubchem.ncbi.nlm.nih.gov/compound/Riboprine⟩ (last Accessed 14 August 2022).
Rabie, A.M., 2021a. Teriflunomide: A possible effective drug for the comprehensive treatment of COVID-19. Curr. Res. Pharmacol. Drug Discovery 2, 100055. https://doi.org/10.1016/j.crphar.2021.100055.
Rabie, A.M., 2021b. Cyanorona-20: The first potent anti-SARS-CoV-2 agent. Int. Immunopharmacol. 98, 107831. https://doi.org/10.1016/j.intimp.2021.107831.
Rabie, A.M., 2021c. Two antioxidant 2,5-disubstituted-1,3,4-oxadiazoles (CoViTris2020 and ChloViD2020): successful repurposing against COVID-19 as the first potent multitarget anti-SARS-CoV-2 drugs. New J. Chem. 45 (2), 761–771. https://doi.org/10.1039/D0NJ03708G.
Rabie, A.M., 2021d. Potent toxic effects of Taroxaz-104 on the replication of SARS-CoV-2 particles. Chem.-Biol. Interact. 343, 109480. https://doi.org/10.1016/j.cbi.2021.109480.
Rabie, A.M., 2021e. Discovery of Taroxaz-104: The first potent antidote of SARS-CoV-2 VOC-202012/01 strain. J. Mol. Struct. 1246, 131106. https://doi.org/10.1016/j.molstruc.2021.131106.
Rabie, A.M., 2022a. Potent Inhibitory Activities of the Adenosine Analogue Cordycepin on SARS-CoV-2 Replication. ACS Omega 7 (3), 2960–2969. https://doi.org/10.1021/acsomega.1c05998.
Rabie, A.M., 2022b. Efficacious Preclinical Repurposing of the Nucleoside Analogue Didanosine against COVID-19 Polymerase and Exonuclease. ACS Omega 7 (25), 21385–21396. https://doi.org/10.1021/acsomega.1c07095.
Rabie, A.M., Abdalla, M., 2023. Evaluation of a series of nucleoside analogs as effective anticoronaviral-2 drugs against the Omicron-B.1.1.529/BA.2 subvariant: A repurposing research study. Med. Chem. Res. 32 (2), 326–341. https://doi.org/10.1007/s00044-022-02970-3.
Raj, V., Lee, J.-H., Shim, J.-J., Lee, J., 2022. Antiviral activities of 4H-chromen-4-one scaffold-containing flavonoids against SARS–CoV–2 using computational and *in vitro* approaches. J. Mol. Liq. 353, 118775. https://doi.org/10.1016/j.molliq.2022.118775.
Raj, V., Park, J.G., Cho, K.-H., Choi, P., Kim, T., Ham, J., Lee, J., 2021. Assessment of antiviral potencies of cannabinoids against SARS-CoV-2 using computational and *in vitro* approaches. Int. J. Biol. Macromol. 168, 474–485. https://doi.org/10.1016/j.ijbiomac.2020.12.020.
Smith, E.C., Blanc, H., Surdel, M.C., Vignuzzi, M., Denison, M.R., 2013. Coronaviruses Lacking Exoribonuclease Activity Are Susceptible to Lethal Mutagenesis: Evidence for Proofreading and Potential Therapeutics. PLoS Pathog. 9 (8), e1003565. https://doi.org/10.1371/journal.ppat.1003565.
Tardif, J.-C., Bouabdallaoui, N., L'Allier, P.L., Gaudet, D., Shah, B., Pillinger, M.H., Lopez-Sendon, J., Da Luz, P., Verret, L., Audet, S., Dupuis, J., Denault, A., Pelletier, M., Tessier, P.A., Samson, S., Fortin, D., Tardif, J.-D., Busseuil, D., Goulet, E., Lacoste, C., Dubois, A., Joshi, A.Y., Waters, D.D., Hsue, P., Lepor, N.E., Lesage, F., Sainturet, N., Roy-Clavel, E., Bassevitch, Z., Orfanos, A., Stamatescu, G., Grégoire, J.C., Busque, L., Lavallée, C., Hétu, P.-O., Paquette, J.-S., Deftereos, S.G., Levesque, S., Cossette, M., Nozza, A., Chabot-Blanchet, M., Dubé, M.-P., Guertin, M.-C., Boivin, G., for the COLCORONA Investigators, 2021. Colchicine for community-treated patients with COVID-19 (COLCORONA): a phase 3, randomised, double-blinded, adaptive, placebo-controlled, multicentre trial. Lancet Respir. Med. 9 (8), 924–932. https://doi.org/10.1016/S2213-2600(21)00222-8.
The Washington Post. Understanding omicron's many mutations. Available from: ⟨https://www.washingtonpost.com/health/2021/12/16/omicron-variant-mutations-covid⟩ (last Accessed 18 July 2022).
Wang, X., Cao, R., Zhang, H., Liu, J., Xu, M., Hu, H., Li, Y., Zhao, L., Li, W., Sun, X., Yang, X., Shi, Z., Deng, F., Hu, Z., Zhong, W., Wang, M., 2020. The anti-influenza virus drug, arbidol is an efficient inhibitor of SARS-CoV-2 in vitro. Cell Discovery 6, 28. https://doi.org/10.1038/s41421-020-0169-8.
Wang, Y., Chen, L., 2020. Tissue distributions of antiviral drugs affect their capabilities of reducing viral loads in COVID-19 treatment. Eur. J. Pharmacol. 889, 173634. https://doi.org/10.1016/j.ejphar.2020.173634.
World Health Organization. Tracking SARS-CoV-2 variants. Available from: ⟨https://www.who.int/en/activities/tracking-SARS-CoV-2-variants⟩ (last Accessed 27 July 2022).
Yan, V.C., Muller, F.L., 2020. Advantages of the Parent Nucleoside GS-441524 over Remdesivir for Covid-19 Treatment. ACS Med. Chem. Lett. 11 (7), 1361–1366. https://doi.org/10.1021/acsmedchemlett.0c00316.
Zhao, J., Guo, S., Yi, D., Li, Q., Ma, L., Zhang, Y., Wang, J., Li, X., Guo, F., Lin, R., Liang, C., Liu, Z., Cen, S., 2021. A cell-based assay to discover inhibitors of SARS-CoV-2 RNA dependent RNA polymerase. Antiviral Res. 190, 105078. https://doi.org/10.1016/j.antiviral.2021.105078.
Zhao, J., Liu, Q., Yi, D., Li, Q., Guo, S., Ma, L., Zhang, Y., Dong, D., Guo, F., Liu, Z., Wei, T., Li, X., Cen, S., 2022. 5-Iodotubercidin inhibits SARS-CoV-2 RNA synthesis. Antiviral Res. 198, 105254. https://doi.org/10.1016/j.antiviral.2022.105254.